

Morphodynamics of the erosional phase of crevasse-splay evolution and implications for river sediment diversion function



Brendan T. Yuill^{a,*}, Ashok K. Khadka^a, João Pereira^a, Mead A. Allison^{a,b}, Ehab A. Meselhe^a

^a The Water Institute of the Gulf, Baton Rouge, LA, USA

^b Tulane University, New Orleans, LA, USA

ARTICLE INFO

Article history:

Received 30 September 2015

Received in revised form 3 February 2016

Accepted 4 February 2016

Available online xxxx

Keywords:

Crevasse splay

Sediment diversion

Morphodynamics

Delft3D

ABSTRACT

Despite being a primarily depositional landform, a crevasse splay experiences an initial evolutionary phase that is primarily erosional as sediment-laden river water spills from a main river channel and incises a new route through the river banks and levee into an interdistributary basin or floodplain. This phase sets the dimensions and the conveyance properties of the crevasse, which, in turn, influences the continued expansion or closure of the crevasse channel. However, little is known about the controlling morphodynamics or how the erosional processes transition to depositional processes during this phase. The objective of this study is to investigate these phenomena at the West Bay sediment diversion (Louisiana, USA) using coupled field observations and numerical modeling. The West Bay diversion was cut into a lower Mississippi River levee to mimic the function of a crevasse-splay, i.e., to divert river water and sediment to an adjacent receiving basin for land-building purposes. Bathymetric measurements show that the diversion channel experienced significant natural morphologic evolution during the initial decade (2004–2014). Hydrodynamic and sediment transport modeling suggests that this evolution initially increased the discharge of flow and sediment through the crevasse as the channel became wider and deeper and altered its orientation relative to the main river flow direction. After 5 years, the model results predict that further evolution led to monotonically reduced diversion discharges. During this time, natural and engineered sediment deposition in the receiving basin decreased predicted basin-flow velocities and promoted a backwater effect that reduced the sediment transport capacity of the diversion channel. Observations during the final 2 years show that much of the initial erosion around the diversion had abated indicating that diversion morphology may have stabilized. A modeling sensitivity analysis confirmed that the observed changes to channel geometry and orientation likely promoted flows of water and sediment through the diversion while increases in basin-bed elevation would have had a contrary effect. The morphodynamic evolution of the West Bay diversion documented in this study presents a model indicative of the erosional phase of crevasse-splay evolution in a deltaic distributary fluvial network. Study results offer an analogue on how an engineered river sediment diversion constructed for coastal restoration may function during its first years of operation and suggest that the desired land-building processes may take time to become established.

© 2016 Elsevier B.V. All rights reserved.

1. Introduction

A crevasse splay is a depositional landform created by the diversion of river water and sediment from its channel into a proximal coastal or lacustrine basin or floodplain (North and Davidson, 2012). In natural fluvial systems, the diversion typically is initiated by flooding flows that overtop the channel banks and is maintained by the erosion of a new distributary channel (i.e., the crevasse) through the main channel bank and levee. A fraction of the river sediment will be transported through the crevasse by flow and become deposited after separation from the main river current. This sediment deposition, which forms a discrete sediment package (i.e., the splay), results from an array of

factors that affect the sediment-laden flow as it transitions from the main river channel to the proximal interdistributary basin or floodplain (Welder, 1959; Pizzuto, 1987; Cahoon et al., 2011; Fagherazzi et al., 2015). These factors include a loss of flow energy, decreased flow depth, and an increase in hydraulic roughness. The lifespan of the crevasse is primarily dependent on the balance between the flow sediment-transport capacity within the crevasse and the amount of river sediment diverted into the crevasse inlet (Kleinhans et al., 2008, 2013; Sloff and Mosselman, 2012). Splay growth, because of the gradual influx of and deposition of river sediment, typically leads to a loss of transport capacity within the crevasse by decreasing the crevasse bed slope as the splay sediment progressively aggrades and backfills upstream into the channel. This sediment aggradation within the crevasse leads to eventual closure of the crevasse and a discontinuation of the splay sediment supply (Coleman et al., 1969, 1998; Roberts, 1997). In

* Corresponding author.

E-mail address: brendan.yuill@gmail.com (B.T. Yuill).

certain cases, e.g., when the crevasse slope is much greater than the main channel slope (Slingerland and Smith, 1998), the crevasse sediment-transport capacity may increase relative to the supply of river sediment entering the crevasse leading to erosion of the crevasse bed sediment. Progressive erosion within the crevasse can lead to incision and extension of the crevasse channel into the downslope basin or floodplain and eventual avulsion of the main river channel to a new course at the crevasse location. The wide range process-based and historical studies have found that crevasse-splay formation is a primary control of [i] distributary-channel network evolution (Allen, 1964; Roberts, 1997; Stouthamer, 2001; Edmonds and Slingerland, 2007; Jerolmack and Mohrig, 2007), [ii] a key catalyst of delta lobe building (Coleman and Gagliano, 1964; Kleinhans et al., 2010; Coleman et al., 1998; Fagherazzi et al., 2015), and [iii] a reliable indicator of a rapidly aggrading fluvial system in the stratigraphic record (Smith and Smith, 1980; Bristow et al., 1999; Stouthamer and Berendsen, 2001; Kleinhans et al., 2012). Crevasse splay deposits also have been found to have significant economic importance owing to their collocation with hydrocarbon and coal reserves (Fielding and Crane, 1987; Gundersø and Egeland, 1990).

Crevasse splays are considered depositional features; however, past observations have indicated that the initial phase of their evolution may be primarily erosional in and around the point of flow bifurcation (Bridge, 1984; Florsheim and Mount, 2002; Makaske et al., 2002; Cahoon et al., 2011). In this phase, the overbank floodwater incises the crevasse channel through the bank and levee substrate. The incision is hypothesized to be promoted by (at least) two factors (Kleinhans et al., 2013). The first factor is the initial gradient between the surface-water elevation of the river water and the distal margins of the overbank water (Cahoon et al., 2011). This differential creates a relatively large gradient in energy head (i.e., the energy slope), which leads to flow acceleration and locally enhanced sediment-transport capacity in the flow as it exits the main river channel. An additional factor is the low sediment loads in the flood water because of its extraction from a relatively high position within the vertical profile of the river (Meselhe et al., 2012). For most river flows, sediment concentrations are significantly vertically stratified throughout the flow column and lowest at the water surface. Despite the importance of this early phase in setting the crevasse size and the ultimate sediment transport capacity of the crevasse (and therefore its probable lifespan) (Wells and Coleman, 1987; Dean et al., 2014) little is known about the controlling morphodynamic processes including how crevasse incision abates and how the depositional processes of splay development (and general land building) initiate. The majority of research on crevasse splay evolution (e.g., O'Brien and Wells, 1986; Tye and Coleman, 1989; Bristow et al., 1999; Florsheim and Mount, 2002; Tooth, 2005; Wellner et al., 2005) focus on analyses of deposited river sediments that, theoretically, only fully initiate after the erosional phase has abated. Further, crevasse-splay studies tend to characterize causal processes from the interpretation of relict deposits that, owing to their nature, cannot accurately capture time-varying geomorphic signals from erosional periods (Sadler, 1981; O'Brien and Wells, 1986; Strong and Paola, 2008).

Engineered river sediment diversions are mechanically constructed to mimic the geomorphic function of a natural crevasse splay, i.e., the conveyance of sediment-laden river water to proximal interdistributary basins to promote sediment deposition and land building (Paola et al., 2011; Dean et al., 2014). This method of land building has garnered significant interest by state and federal agencies along the Gulf Coast of the United States of America (USA) as a means to mitigate Mississippi River delta land loss promoted by relatively high regional rates of wetland erosion and subsidence (e.g., CPRA, 2012; DeLuca, 2014) despite the fact that few analogous projects exist from which performance may be predicted. While an increasingly large number of studies have sought to assess the land-building potential of sediment diversions, they have tended to extrapolate long-term potential as a simple function derived from observations of discrete events (e.g., Lane et al., 2001; Snedden

et al., 2007; Nittrouer et al., 2012; Allison et al., 2013; Falcini et al., 2012) or from generalized receiving basin properties and initial conditions (e.g., Kim et al., 2009; Blum and Roberts, 2009; Boustany, 2010; Wamsley, 2013; Dean et al., 2014). However, in cases where aspects of the diversion are left fully or partially uncontrolled, which may be advantageous to limit construction and maintenance costs (Turner and Boyer, 1997; Kemp et al., 2014) or to keep diversion operations more aligned with natural processes (Kellerhals et al., 1979; Allison and Meselhe, 2010), the applicability of the results of these studies are unknown. If sediment diversions act similar to natural crevasse splays through their lifespan, they may experience considerable evolution, especially during an initial erosional phase, which may alter their ability to convey river flow and sediment as well as their long-term land-building potential.

This study examines the morphodynamics of an engineered crevasse splay (the West Bay diversion, Louisiana, USA) during the first 10 years (2004–2014) after it was cut through the levee of a large, low-slope, sand-bed river (i.e., the lower Mississippi River). The first study objective is to document the observed evolution of the crevasse-splay morphology during the study period and to investigate how this evolution affected hydrodynamics and sediment transport within the crevasse channel. Additional study objectives include identification of the relative influence of key morphologic properties on the observed crevasse-splay evolution and the construction of a conceptual model of the initial phase of crevasse-splay evolution using a synthesis of study results and existing geomorphic theory. A final study objective is to investigate how the morphodynamics (observed and predicted) at the West Bay diversion might influence river sediment diversion function generally. In the context of this study, 'sediment diversion function' refers to the ability of the diversion to divert and convey river flow and sediment into a proximal receiving basin. This study uses a combination of field observations and numerical modeling in an attempt to achieve these objectives.

2. Study area

The West Bay sediment diversion (Fig. 1) is located within the west bank of the lower Mississippi River (LMR) channel at the upstream margins of a large, lateral channel sand bar, 7.6 km upstream of the Head of Passes, i.e., located at river kilometer (RK) 7.6. At the time of its construction by the U.S. Army Corps of Engineers (USACE) in late 2003, 12% of the 50-km² receiving basin was emergent marsh while the rest was shallow (water depths <3 m) open water (Carter, 2003). The location of the diversion was selected, in part, because it is the site of an abandoned, natural crevasse-splay complex that was primarily active between 1830 and 1930 (Wells and Coleman, 1987; Kolker et al., 2012). While the deposition of river sediment currently is building sub-aerial land in some localized areas of the LMR delta, the majority of regional marshes are actively deteriorating (Barras et al., 2009).

The diversion channel, as initially constructed, had a measured flow capacity of 396 m³/s when the proximal LMR was at median river stage, i.e., the river stage not exceeded during 50% of the total record of measurement (CPRA Fact Sheet, 2009). The 'as-built' channel width (Fig. 2) was reported as 59.4 m and the bed elevation was −7.3 m NAVD88 (North Atlantic Vertical Datum of 1988). By 2008, natural processes had increased the measured flow capacity of the diversion channel to 765 m³/s at the median river stage (Sharp et al., 2013). The diversion channel was designed to operate as a natural crevasse and left uncontrolled except for stone armoring placed along the riverside bank. By 2009, the rapid growth of the diversion channel dimensions and observations of sediment aggradation (shoaling) within the proximal LMR navigation channel and nearby anchorage (i.e., the Pilottown Anchorage Area) raised concerns with river managers, which resulted in the increased bathymetric and hydrodynamic monitoring of the area (Allison and Meselhe, 2010; Sharp et al., 2013). In fall 2009, the USACE began construction of a series of engineered subaerial islands

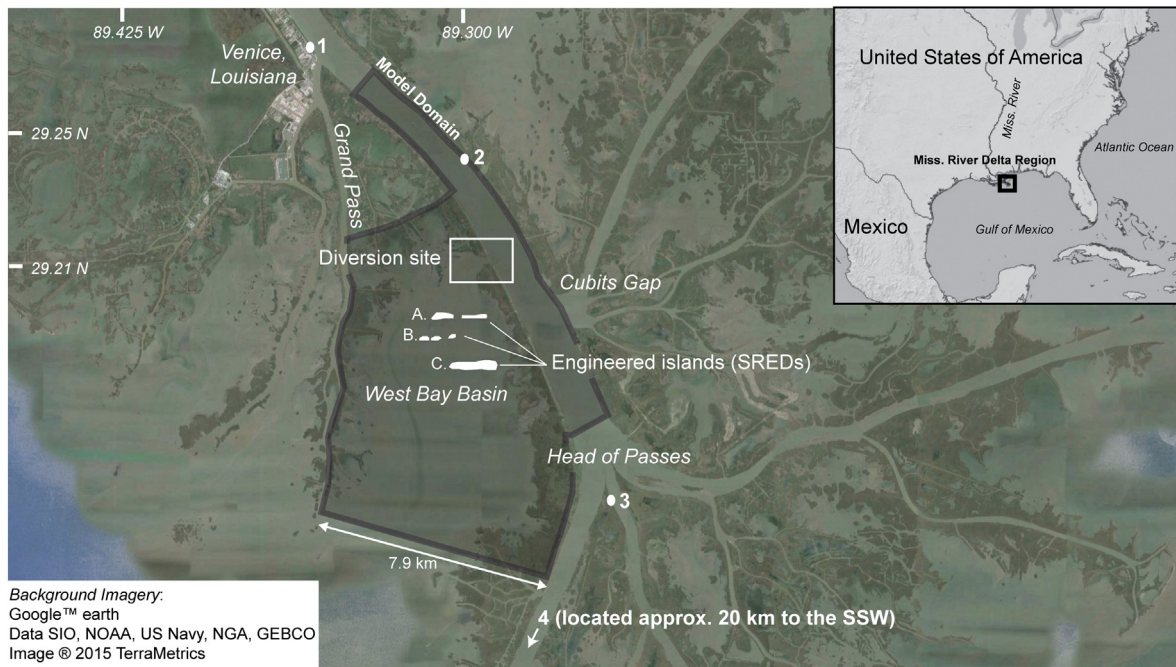


Fig. 1. Map of the study site and numerical model domain (i.e., the shaded polygon). The map also shows the location of the engineered islands (SREDS) within the basin constructed in 2009–2010 (B) and 2013 (A and C). The Venice, West Bay, Head of Passes, and Southwest Pass river stage gauges are designated by points 1, 2, 3, and 4, respectively.

(referred to as ‘sediment retention enhancement devices’ or ‘SREDS’) within the West Bay receiving basin. These islands were constructed out of sandy borrow material dredged from the river navigation channel with the objectives of slowing flow velocities within the diversion channel, limiting the growth of the diversion site, and promoting increased sediment deposition within the basin. Fig. 1 shows the approximate footprints of the SRED islands.

With the study area, the LMR discharge displays seasonal and intraseasonal oscillations, primarily dependent on recent precipitation and snowmelt in its upper tributary basins (i.e., upper Mississippi River basin, the Missouri River basin, the Ohio River basin). With the use of multiple flood-control spillways (e.g., the Old River control structure, the Morganza spillway, the Bonnet Carré spillway), USACE river managers attempt to limit maximum river discharges within the study area to $42,475 \text{ m}^3/\text{s}$ as measured at RK 206 (near the city of New Orleans). The closest permanent river gauge to the study area,

i.e., the U.S. Geological Survey (USGS) station at Belle Chasse, is located at RK 122 and was installed in 2008. The approximate distribution of average-daily discharges measured at that location spans $4000\text{--}35,000 \text{ m}^3/\text{s}$ and has an approximate median value of $15,000 \text{ m}^3/\text{s}$. The USACE operates a river stage gauge at Venice, Louisiana (RK 17.2) that has been in operation since 1953; the minimum and maximum stages recorded are -0.41 and 2.60 m NAVD88 and the average annual range is -0.06 and 1.32 m NAVD88 . The diurnal marine tidal signal extends through the study area; however, the effect on flow velocities has been assumed to be minimal (Nittrouer et al., 2011) due to the low ratio of tidal-prism height ($\sim 0.3 \text{ m}$) to river depth ($> 25 \text{ m}$).

The bed material of the LMR is spatially and temporally variable depending on local near-bed flow velocities and seasonal fluctuations in sediment supply. Bed-material textures generally range from unconsolidated muds, found primarily in slack-water areas during low seasonal discharges, to medium sands (Galler and Allison, 2008). Bed sands

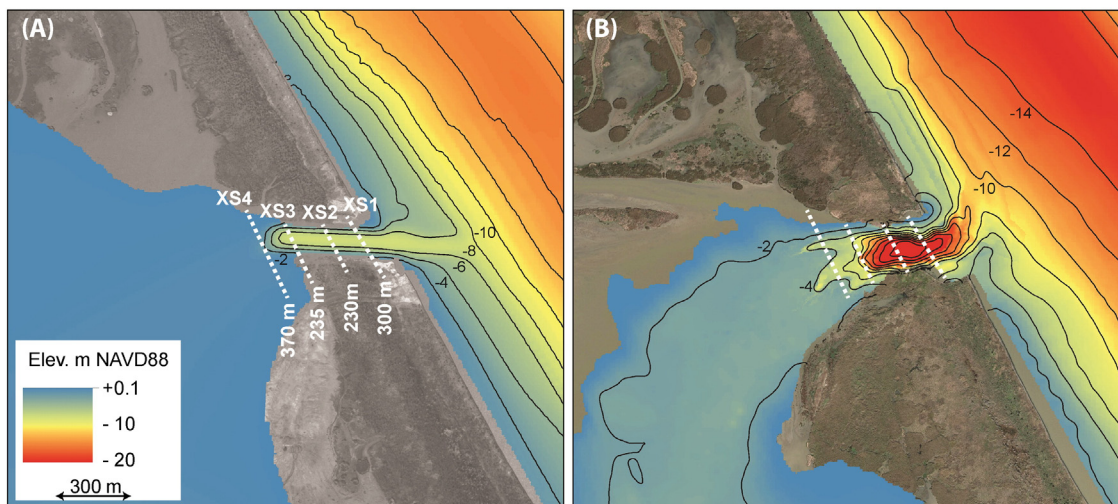


Fig. 2. Bathymetric maps for the West Bay diversion, (A) 2004 and (B) 2014. Contour lines delineate elevation change at 2-m intervals. Also shown are the location and width for four reference cross sections used to examine model velocities within the diversion channel. These maps were created from bathymetric data reported in the results section of this manuscript.

transported within the active layer often compose bedforms on the order of meters thick and tens of meters long (Ramirez and Allison, 2013). Sands below the active layer typically appear well mixed and may range from <1 to 5 m thick in the main channel and >10 m thick within channel bars. Sediment transport studies performed upstream of the study area (+50 km) have found that significant sand transport does not initiate until river discharges exceed 10,000 m³/s. From a seasonal perspective, peak rates of sediment transport typically precede the first annual hydrograph peak (Mossa, 1996; Allison et al., 2012). The degree of antecedence is promoted by sediment hysteresis and increases with the magnitude of the hydrograph.

As an existing analogue, the West Bay river diversion is one of only a few locations that offer insight into geomorphic behavior of future engineered river diversions along the Mississippi River delta (Allison and Meselhe, 2010). This insight is extremely valuable for future coastal restoration initiatives; the State of Louisiana has initiated feasibility studies to locate, design, and operate new river sediment diversions (CPRA, 2012; Peyronnin et al., 2013) to promote land building and to mitigate coastal marsh loss. The area of marshland surrounding the Mississippi River delta is declining at rates exceeding 25 km²/year because of natural processes (e.g., sediment compaction) and anthropogenic activity (e.g., levee and canal construction; Roberts, 1997; Day et al., 2007). Recent studies investigating optimal sediment-diversion design along the lowermost Mississippi River, in terms of land-building potential, suggest that diversion dimensions should accommodate at least 1500 m³/s of river discharge (Wang et al., 2014) and should be located adjacent to channel sand bars (Allison et al., 2014). The West Bay diversion is located near a large channel bar but its typical discharge is likely <1500 m³/s. However, existing alternative diversion analogues either discharge significantly less flow and sediment (e.g., the Davis Pond or Caernarvon diversions) or are located in fluvial systems with significantly different flow and sediment transport regimes (i.e., the Bonnet Carré spillway, Wax Lake delta, Louisiana, USA) relative to the planned sediment diversions (Bentley et al., 2014).

3. Methods

Study methods include a combination of observational data analyses and numerical modeling. The observational data were derived from archival sources and from new field measurements. The observational bathymetric data were used to characterize the morphological evolution of the field site, and the observational flow velocity and sediment transport data were used to parameterize and calibrate a computational morphodynamic model. Numerical modeling was used to estimate hydrodynamics and sediment transport flux within the study area at spatial and temporal resolutions greater than that available from observational measurements.

3.1. Observational measurements

3.1.1. USACE flow velocity, sediment concentration, and river stage data collection

The USACE Engineer Research and Development Center (ERDC) collected a series of flow velocity measurements within the West Bay diversion channel and the proximal river reach using a boat-based acoustic Doppler current profiler (ADCP; Sharp et al., 2013). Approximately 7 different velocity surveys were conducted between 2009 and 2011 with various spatial extents (typically 5–10 cross section transects were performed during a survey). The ADCP instrument was manufactured by RD Instruments, Inc. (RDI; www.rdinstruments.com) and operated at either 600 or 1200 kHz depending on the relative turbulence of the river flow. Channel discharges were calculated from the velocity data at each transect using RDI WinRiver II software. Velocity measurements were automatically georeferenced during collection using an inertial positioning system (Applanix POS MV) and satellite guidance (i.e., GPS). A complimentary data set of diversion discharge

was calculated by the USACE New Orleans District using additional ADCP measurements at the mouth of the diversion channel. This data set was composed of total discharge values calculated from 90 individual surveys between January 2004 and December 2012. In conjunction with the flow velocity measurements, USACE ERDC also collected isokinetic sediment-concentration samples, using a US P-6 point integrating suspended-sediment sampler at stations within the diversion mouth and at main channel locations immediately upstream of the diversion. At each station, sediment concentration was measured at five standardized depths along the vertical flow profile (using the methodology of Edwards and Glysson, 1988). Laboratory grain-size analysis was performed on the collected sediment samples using laser diffraction. For the purposes of this study, the measurements of flow velocity and sediment were used to calibrate the numerical model employed to calculate diversion discharges (discussed later in this section). A modeling approach was necessary because no observed velocity or sediment data were available for analysis from within the study area during the first five years of diversion operation.

Surface-water elevation was measured at daily intervals (at 800 local time, 1300 GMT) within the study area at four USACE stage gauges: Mississippi River at Venice (gauge ID = 01480), Mississippi River at West Bay (01515), Mississippi River at Head of Passes (01545), and Mississippi River Southwest Pass 7.5 BHP (01575). The data sets were accessed at <http://rivergages.mvr.usace.army.mil>. A linear-regression analysis was performed using the daily Venice stage gauge data and the USACE New Orleans District discharge data set to extrapolate daily river discharge values throughout the study period. Surface-water elevations recorded at the Head of Passes and Southwest Pass gauges were used to populate boundary conditions for numerical modeling. Surface-water elevations recorded at the West Bay gauge were used for numerical model calibration.

3.1.2. Bathymetry collection

Boat-based bathymetric surveys of the diversion channel were conducted in 2004, 2005, 2009, 2011 (partial coverage), 2012, and 2014. The 2009 survey extended over the entire river-channel bed between Venice and the Head of Passes. Surveys executed between 2004 and 2009 were conducted by USACE survey teams using a hull-mounted, side-scan, interferometric swath sonar (i.e., a GeoAcoustics GeoSwath Plus 250 kHz). The 2012 and 2014 surveys were conducted by Water Institute of the Gulf scientists using a multibeam swath sonar (i.e., Reson SeaBat 7125 400 kHz). Both instruments utilized positioning data acquired using an Applanix POS MV and a real-time kinematic (RTK) global-positioning system (GPS), which provided vertical accuracies to within 2–4 cm. Each survey data set was post-processed using HYPACK (www.hypack.com) or Caris (www.caris.com) software to produce a 1-m² cell-size digital elevation model (DEM) representing the diversion channel bathymetry. Further information about the multibeam data collection methods can be found in Ramirez and Allison (2013).

Subaerial terrain extent and shorelines around the diversion channel were approximated using high-resolution aerial imagery available from Google Earth Pro (www.google.com/earth); aerial imagery was available for the following time periods: 2004, 2005, 2009, 2012, and 2014. The elevation of the subaerial terrain within the study area was assumed to have been relatively stable over the study period and was estimated from a 2011 aerial LiDAR survey (~1-m² horizontal resolution, accessed at <http://earthexplorer.usgs.gov>).

The bathymetry of the West Bay receiving basin was surveyed in 2003, 2009, 2011, and 2014. The 2003 through 2011 surveys were collected by the State of Louisiana using RTK GPS (Andrus, 2007). Each survey consisted of the reoccupation of 17 transects stretching the full basin width, oriented transverse to the mean direction of flow (i.e., WNW to ESE). Transects were spaced between 300 and 475 m apart. Within each transect, elevation was measured at elevation breakpoints (with a 60-m maximum allowable spacing). The 2014

survey was conducted by the Water Institute of the Gulf and consisted of measurements made with either an RTK GPS (i.e., Trimble R6 RTK system), boat-based single-beam sonar (i.e., Odom Hydrographics Hydrotrac single-beam, 200 kHz shallow-water fathometer) or a boat-based LiDAR (i.e., Dynascan M150 coupled with the Applanix POS MV positioning system) dependent on local flow depth. The 2014 survey attempted to capture basinwide elevation breakpoints and did not follow the same transect routes as the previous surveys. The minimum vertical resolution produced by this survey method at a data collection point was 4.5 cm.

3.1.3. DEM production and analysis

To produce a time series of bathymetric data sets representing the continuous morphology of the West Bay diversion channel, West Bay receiving basin, and the proximal river channel, river survey data were combined with receiving basin and terrain data in the ArcGIS (www.ESRI.com) desktop environment. Composite DEMs representing the following years were produced: 2004 (using the 2003 receiving basin survey and the 2004 diversion channel surveys), 2009 (using the 2009 receiving basin and diversion surveys), 2012 (using the 2011 receiving basin and 2012 diversion survey), and 2014 (using the 2014 receiving basin and diversion survey). The composite DEMs were computed using the inverse-distance weighting method to interpolate point elevation measurements into a continuous surface. The final DEM resolution was set at 5 m, which required downscaling of receiving basin bathymetric data (using linear interpolation) and upscaling of diversion channel bathymetric data (using spatial averaging), to fit the maximum-required resolution of the numerical model grid (discussed later in this section).

The final DEMs used to populate the depth values of the numerical model employed a single static bathymetry derived from the 2009 multibeam survey for the river bed outside of the immediate diversion site (i.e., >500 m from the diversion inlet). This was to prevent changes in the river bed unrelated to the evolution of the diversion channel from affecting the numerical model results.

To calculate metrics of channel-averaged geometry (e.g., width, depth), measurements were derived from the composite DEMs at visually defined breakpoints in channel morphology (at 4–10 cross sections per survey) and averaged together to calculate single metric values per time interval, such as mean channel width, mean channel depth, and hydraulic radius. The metrics were computed in reference to a single, uniform surface-water elevation approximate to the regional mean low-water tidal datum (0.1 m NAVD88). Mean channel orientation was estimated by fitting a linear trend line to the shoreline of each diversion bank as identified by aerial imagery and then by calculating the average orientation of the two lines.

3.2. Numerical modeling

3.2.1. Model overview

Flow and sediment transport were simulated using Delft3D (Lesser et al., 2004), an open-source multidimensional sediment and hydrodynamics modeling package. Delft3D computes flow using the Navier-Stokes equations of fluid motion and sediment transport by solving the continuity and transport equations on a two- or three-dimensional curvilinear finite-difference grid. Turbulence is simulated using a range of possible closure schemes (e.g., k-Epsilon). The Delft3D code is well documented (<http://oss.deltares.nl/web/delft3d>), and it is routinely used by the research community to model river morphodynamics (e.g., Matsubara and Howard, 2014; Schuurman and Kleinans, 2015).

The objective of the initial Delft3D model experiment was to estimate the three-dimensional (3D) flow and sediment transport fields in and around the sediment-diversion channel based on a suite of steady river discharges prescribed at the upstream boundary of the LMR. A 3D numerical modeling approach was used by this study so that depth-dependent flow structures, which are likely important to

diversion hydrodynamics (Neary and Odgaard, 1993), could be resolved in addition to depth-averaged hydrodynamics.

3.2.2. Model set up

To simulate 3D river hydrodynamics in the study area, a computational grid was fitted to the geometry of the study area (shown in Fig. 1). The model domain within the river extended from the LMR Head of Passes to RK 13.8. Within the receiving basin, the model domain was bounded by Grand Pass, the western levee of the Mississippi River, Southwest Pass, and extended south ~10 km downstream of the diversion location. The grid-cell dimensions varied spatially within the model domain, from 80 m by 400 m at the open-water boundaries to 5 m by 5 m around the diversion channel. The vertical grid structure was composed of 20 vertical layers. The layer thicknesses were defined as a fraction of the total flow depth and were stratified parabolically with higher resolution near the bed. The total grid height was dependent on the locally calculated river stage. The model domain had five primary open boundaries: the upstream river boundary, the downstream river boundary (approaching the Head of Passes), the Cubit's Gap river outlet, the Grand Pass receiving basin inlets, and the West Bay receiving basin outlet. The Grand Pass inlets were composed of 11 relatively small channels that introduced river flow and sediment into the West Bay receiving basin via Grand Pass instead of the West Bay diversion. Flow through the Cubit's Gap and Grand Pass boundaries was predicted as a fraction of the river discharge through the upstream boundary (~15% and 8%, respectively). The flow through the downstream river boundary was set as a water-level boundary condition based on the results of a regression analysis using estimated river-discharge data at Venice (Q_{US}) and daily water-elevation measurements collected at the Head of Passes stage gauge, i.e., stage (m NAVD88) = $1 \times 10^{-5} Q_{US} + 0.39$. Flow through the West Bay basin outlet was set as a static water-level boundary condition (0.39 m NAVD88) and was assumed to have been controlled by mean sea level rather than river discharge.

Two types of scenarios were modeled: the 'observed bathymetry' scenarios, which employed the composite 2004, 2009, 2012, and 2014 DEMs to populate the bed elevation of the model grid cells; and the 'synthetic bathymetry' scenarios, which employed a modified version of the composite 2004 DEM. The only difference between each modeled scenario in all cases was bathymetry.

In each scenario, three different 'steady-state' hydrodynamic environments were simulated by introducing three different discharges at the upstream river boundary and adjusting the downstream boundaries accordingly. The three discharges typify a low (8800 m³/s), moderate (15,600 m³/s), and high (21,000 m³/s) discharge for the LMR within the study area. To model a steady flow, Delft3D was run using non-time-varying boundary conditions until an approximate steady-state condition was achieved. To simulate sediment transport the model employed the van Rijn et al. (2001) transport function, which calculates bedload and suspended sediment transport separately. Sediment transport was computed for three sand grain sizes (very-fine, fine, and medium sand that were modeled as 0.063, 0.125, and 0.250 mm in diameter, respectively) that typify the range of sand grain sizes observed in the suspended and bed material load within the lower Mississippi River (Thorne et al., 2000). Sediment finer than sand was not expected to significantly contribute to the initial stages of land building (Dean et al., 2014) and was neglected in this study for simplicity.

Additional model parameters were set during calibration tests that employed an observed high-resolution survey of the flow field in and around the diversion site using a boat-based ADCP at the approximate 'moderate' river discharge. The hydraulic bed roughness of the model domain (in terms of the Manning's roughness coefficient, n) was set based on calibration test results. Optimal calibration was obtained when $n = 0.020$ in the river channel and $n = 0.028$ in the diversion channel. Once parameterized, model performance was retested using ADCP transect data collected within the diversion channel at low and high discharge. Calibration tests used bathymetric and ADCP velocity

data acquired in 2009. A detailed description of model parameterization and calibration methods is included in the online supplemental material.

3.2.3. Observed bathymetry scenarios (OBS)

The objective of the OBS model runs (Table 1) was to investigate how the changes in diversion channel and receiving basin morphology affected the diversion function (i.e., the ability of the diversion to convey river water and sediment into the receiving basin). The OBS utilized the four composite DEMs derived from observed bathymetric observations (i.e., 2004, 2009, 2012, and 2014) and three steady river discharges (low, moderate, and high). The primary model results analyzed from these scenarios were [i] flow velocity at four diversion channel cross sections (cross section locations are shown in Fig. 2); [ii] the total discharge of water and sand passing through the diversion channel; and [iii] maps of depth-averaged flow velocity, boundary shear stress (referred to as ‘bed stress’ in Delft3D nomenclature and hereafter in this manuscript), and surface-water elevation throughout the model domain.

3.2.4. Synthetic bathymetry scenarios (SBS)

The objective of SBS model runs was to investigate the relative effect of specific morphologic properties on the diversion function. In these numerical experiments, the same Delft3D model (i.e., the same parameters and boundary conditions) employed in the OBS was run using a single bathymetry that was systematically modified to vary one morphological property. Fourteen scenarios were run that iteratively varied one of three different morphological properties: channel geometry, channel orientation, and basin bed elevation. The morphological properties were varied by making idealized modifications to the observed 2004 composite DEM before each model run.

To explore the impact of diversion channel geometry on diversion function, five different scenarios (i.e., SBS 1 through SBS 5 in Table 1) were run with a uniformly shaped trapezoidal diversion channel in place of the observed channel. During this experiment, channel geometry was classified using a single parameter, hydraulic radius (R), for simplicity. In each of the five model runs either the mean channel width or depth was varied to produce a unique R value.

The impact of channel orientation on diversion function was examined by running five model scenarios (SBS 6 through SBS 10) using a diversion channel with uniform dimensions and by altering the horizontal channel orientation. For these scenarios, the diversion bed elevation

was set at -7.25 m NAVD88, and the channel width was kept uniform at 105 m.

The impact of the basin-bed elevation on diversion function was examined by running four model scenarios (SBS 11 through SBS 14) using the observed 2004 diversion-channel bathymetry and by adjusting a fraction of the receiving basin-bed elevation by a prescribed uniform amount. This manual adjustment to the basin-bed elevation, which simulates sudden bed-sediment aggradation, was applied before the initial hydrodynamic time step of each model run. During these scenarios, adjusted basin-bed elevations were not permitted to increase above -0.25 m NAVD88 to prevent the blockage of critical flow pathways and the creation of unrealistic flow circulation patterns (bed elevations initially above that elevation were not adjusted). For these scenarios, the diversion bed elevation was -5.25 m NAVD88, the diversion width was kept uniform at 145 m, and the diversion orientation was kept uniform at 275° (in compass degrees). The objective of the experimental scenarios that increased basin-bed elevation was to simulate the backwater effects of sediment aggradation and land building on diversion function. The primary model results analyzed from the SBS were the total discharge of water and sand passing through the diversion channel.

3.2.5. Supplemental synthetic bathymetry scenario (SSBS)

A supplemental synthetic bathymetry scenario was run to explore the modeled effect of the engineered SRED islands, built in the receiving basin between 2009 and 2014, on diversion function. In this scenario, the observed 2014 bathymetry was modified by reducing the bed elevation within the subaerial footprint of the SRED islands (as shown in Fig. 1) to -0.5 m NAVD88, which was the approximate mean elevation of the ambient basin bed that was assumed not significantly affected by SRED construction.

4. Results

4.1. Observations of flow and sediment transport

Analysis of the USACE discharge data (Fig. 3A) indicates that the West Bay sediment diversion captured an average of 7.7% of the LMR discharge approaching the diversion site. This percentage increased from 6.0% during the first half of the study period (2004–2008) to 9.5% during the second half of the study period (2009–2014). The LMR discharge exhibited no linear temporal trend over the study period and had a median observed value of 8877 m³/s. Fig. 3B shows the distribution of river-stage values measured at the Venice gauge for the study period divided into three intervals: 2004–2009, 2009–2012, and 2012–2014 (i.e., the intervals between bathymetric surveys of the diversion channel). The 2009–2012 interval experienced a greater frequency of higher river stages (and discharges) than the other intervals because of the unusually large spring flood in 2011, which was the flood of record for the LMR. Fig. 3B also shows the frequency of the three modeled river discharges modeled for this study estimated from regression of the USACE discharge measurements and the Venice stage gauge data.

Sediment transport data collected by the USACE in 2009 are shown in Fig. 4. Marginal increases in flow result in a similar increase in suspended-sediment transport for the LMR and for the diversion channel suggesting that, during that time period the amount of the sediment entering the diversion was predominately controlled by river processes. The fraction of the suspended sediment composed by sandy sediment was similar in the river and in the diversion channel, typically varying between 5 and 40% and increased with river discharge.

4.2. Observations of geomorphic changes within the diversion channel and receiving basin

The diversion channel experienced significant morphological change from its initial (‘as-built’) state in 2004 to that observed in

Table 1
List of numerical modeling scenarios.

Scenario ID	Dependent parameter	Dependent parameter value
OBS 1	Bathymetry	Observed 2004
OBS 2	Bathymetry	Observed 2009
OBS 3	Bathymetry	Observed 2012
OBS 4	Bathymetry	Observed 2014
SBS 1	Diversion channel R^a	3.5 m (160/5) ^b
SBS 2	Diversion channel R	6.1 m (80/12)
SBS 3	Diversion channel R	6.3 m (160/9)
SBS 4	Diversion channel R	8.4 m (160/12)
SBS 5	Diversion channel R	12.8 m (160/20)
SBS 6	Diversion channel orientation	270°
SBS 7	Diversion channel orientation	265°
SBS 8	Diversion channel orientation	255°
SBS 9	Diversion channel orientation	247.5°
SBS 10	Diversion channel orientation	240°
SBS 11	Basin bed elevation	Obs. 2004 + 0 m = OBS 1
SBS 12	Basin bed elevation	Obs. 2004 + 0.25 m
SBS 13	Basin bed elevation	Obs. 2004 + 0.5 m
SBS 14	Basin bed elevation	Obs. 2004 + 1.0 m
SSBS	Basin bed elevation	Obs. 2014 – SREDS

^a R = hydraulic radius

^b Value in parentheses is channel-averaged width/depth ratio.

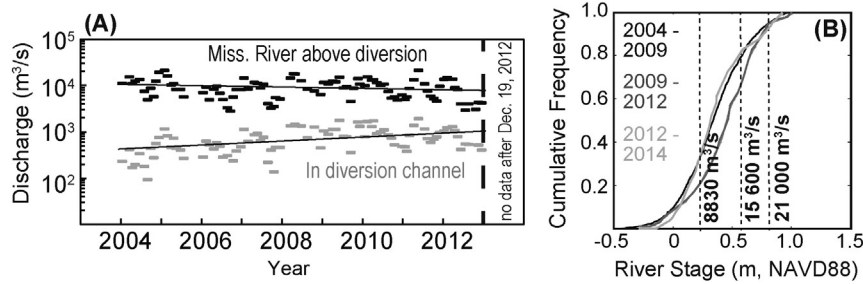


Fig. 3. (A) ADCP-derived channel discharge for the Mississippi River immediately upstream of the diversion and within the diversion channel; linear trend lines are fitted to the discharge data at each location. (B) The cumulative frequency distributions for Mississippi River stage measured near Venice, Louisiana, for three time periods. The approximate average stages for three river discharges are also shown.

2014 (Fig. 2; Table 2). The channel increased in width and depth between each survey until 2012; the channel depth increased faster than channel width, in terms of percentage of the initial length, which decreased the width-to-depth ratio and increased the hydraulic radius. Hydraulic radius is a common metric of flow efficiency (Henderson, 1966) that correlates to increased flow and sediment discharge (holding all other variables constant). Between 2012 and 2014, the channel width remained relatively stable, while the mean channel depth decreased. Throughout the period of observation, the most pronounced elevation change observed in the diversion channel bed was due to the development of, and subsequent infilling of, a large scour hole along the channel thalweg (Fig. 5).

Fig. 6 shows maps of observed bed-elevation change for the three intersurvey periods: 2004–2009, 2009–2012, and 2012–2014. Between the initial channel construction in 2004 and 2009, the entire bed (except for the main river channel bed immediately downstream of the diversion inlet) experienced significant erosion. The highest values of erosion

occurred throughout the central section of the diversion channel, which created a discernable scour hole (shown in profile in Fig. 5). Between 2009 and 2012, the downstream extent of the diversion channel-bed area that experienced erosion was appreciably reduced relative to the previous time interval. Also, the bed along the northern diversion-channel bank remained stable or experienced aggradation. Between 2012 and 2014, the bed area experiencing erosion extended slightly farther into the basin. However, much of the diversion channel bed located around the existing scour hole and the transition zone between the diversion channel and the basin experienced net aggradation.

The diversion channel orientation changed throughout the study period. The angle at which the diversion channel was offset from the main LMR-channel orientation decreased. In 10 years, the channel orientation swung 16° from 275° to 259°; for reference, the approximate mean flow direction of the main river was 148° as it passed the diversion. The channel reorientation reduced the angle at which the river flow was redirected in order to enter the diversion.

Fig. 7 shows the spatially averaged receiving basin bed elevation in respect to distance downstream from the diversion channel outlet. Figure values were computed directly from the time series of receiving basin bathymetric surveys. Generally, for distances <2 km away from the diversion outlet, the basin bed tended to erode over the study period. For distances >2 km, the bed experienced erosion through 2009 and then either aggraded or remained stable through 2014. Bed areas between 2 and 4 km below the diversion outlet were likely affected by SRED island construction starting in 2009.

4.3. Observed bathymetry scenario model results

Numerical modeling results (as summarized in Fig. 8) predicted that, for a given river discharge, the flow and sand load in the diversion channel varied by over 250 and 750%, respectively, because of the evolving diversion morphology. Flow and sand transport within the diversion channel increased from 2004 to 2009 and then gradually declined thereafter. Fig. 9 shows the fraction of the total river flow and sand load that was predicted to enter the diversion channel for the four bathymetries modeled. Increasing river discharge increased the ratio of the fraction of the river sand that was diverted relative to the fraction of the river flow that was diverted. For reference, Fig. 9 shows the 1:1 line where the fraction of diverted river flow and sand load are identical. Essentially, this 1:1 line represents a sediment water ratio of unity implying that the average sand concentration in the diverted water is the same as the average sand concentration in the main river (Meselhe et al., 2012).

The magnitude and distribution of flow velocities in the diversion channel were predicted to vary significantly because of the observed evolution in channel and basin morphology. Fig. 10 illustrates the lateral spatial distribution of depth-averaged flow velocities along four cross sections within the diversion channel. Along the upstream cross sections, the zone of highest flow velocity (i.e., the high-velocity core) shifted south toward the southern (left descending) bank over time.

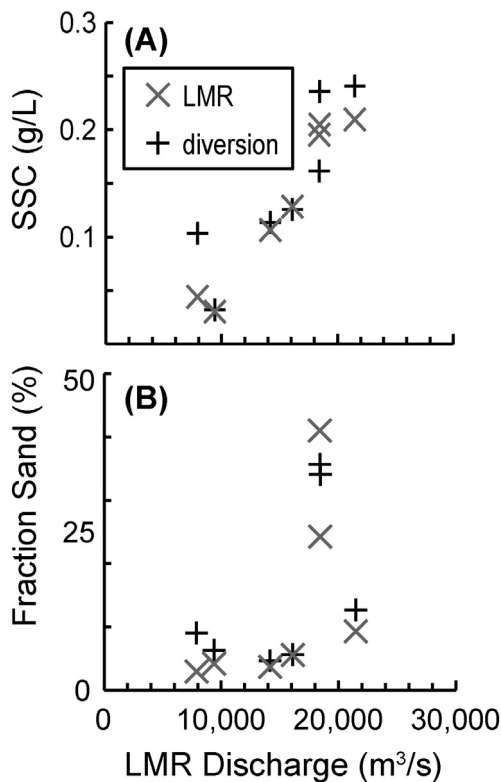


Fig. 4. (A) Observed relationship between river discharge and suspended-sediment concentration (SSC) measured upstream of the diversion inlet at LMR RK 8.4 and in the diversion channel. (B) Shows the fraction of each sediment measurement that was composed of sand (>0.063 mm in diameter). All observed sediment data were collected in 2009 by the USACE ERDC.

Table 2
Summary of morphological adjustments to the diversion channel.

Year	Width (W) m	Depth (D) ^a m	Area m ²	Hydraulic radius m	W/D	Channel orientation Compass deg.	Energy slope ^b m/m
2004	143	5.3/7.6	761	5.3	18.9	275	23.1×10^{-5}
2005	158	5.1/9.6	810	5.1	17.1	270	Not modeled
2009	190	10.7/19.9	2041	10.0	9.9	268	7.2×10^{-5}
2012	204	13.7/27.0	2800	13.0	7.7	262	4.3×10^{-5}
2014	204	12.8/19.5	2614	12.2	10.5	259	2.9×10^{-5}

^a Avg. depth/max depth, depth is measured below predicted mean low sea level = 0.1 m NAVD88.

^b Approximated as diversion water–surface slope while upstream LMR discharge = 15,600 m³/s.

Near the north (right descending) bank, a zone of reverse-flow (i.e., streamwise negative velocity) grew in length and magnitude and was likely composed of a stable eddy-like flow structure. Along the downstream cross sections, flow velocity became more spatially uniform and declined over time, on average. These trends are exemplified in Fig. 11, which shows the predicted 3-D flow patterns at the upstream and downstream end of the diversion channel in 2004 and 2014.

4.4. Synthetic bathymetry scenario modeling results

The SBS model results are summarized in Fig. 12. Because of the negligible sand load discharges predicted for the ‘low’ river discharge, these results were dropped from further analysis. Results from SBS 1–5 (the scenarios investigating the effect of hydraulic radius) show that flow and very-fine sand discharge exhibited a relatively weak, positive relationship with the five modeled *R* values. Discharge of the coarser sand fraction (fine and medium sand) tended to decrease with *R*. For SBS 6–10 (the scenarios investigating channel orientation), flow and sand transport peaked at a 107° angle offset from the main channel orientation (i.e., the bifurcation angle). The scenario that employed a 122° bifurcation angle predicted the lowest discharges; this angle is approximate to the design bifurcation angle of the West Bay diversion. The results from SBS 11–14 (the scenarios investigating the effect of basin elevation) predict that flow and sediment discharge within the diversion channel exhibited a significant, decreasing power-law type relationship with mean receiving basin bed elevation.

5. Discussion

5.1. Morphodynamic evolution of the West Bay diversion

Much of the observed morphologic evolution of the West Bay diversion was likely in response to the spatial variability in the flow velocities as the river water entered and passed through the diversion channel. The diversion channel, as built in 2003, was constructed as a straight channel at a large (obtuse) angle relative to the direction of the main

river flow. The results of the model scenario that employed the 2004 bathymetry (OBS 1) predicted that a large fraction of the cross-sectional area of the flow within the diversion channel was composed of a core of relative high velocity (Fig.11); the proximity of the high velocity core to the channel bed and banks increased the relative susceptibility of those areas to sediment erosion. On account of the relatively uniform geometry of the initially dredged channel, the spatial gradients in flow velocity were initially small; however, as the flow was turned and guided from its course in the main river channel into the diversion

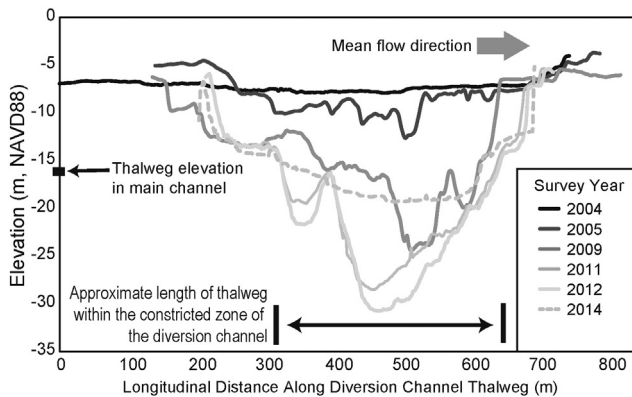


Fig. 5. Thalweg elevations derived from six bathymetric surveys of the diversion channel area.

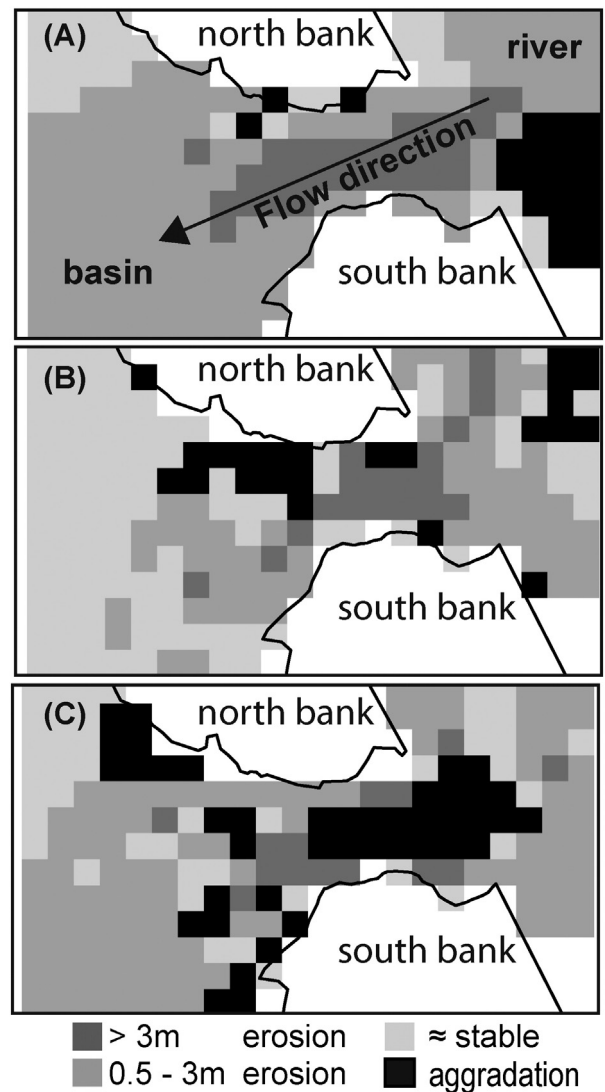


Fig. 6. Observed bed erosion (or aggradation) within the sediment diversion channel for three periods, (A) 2004 to 2009, (B) 2009–2012, and (C) 2012–2014. Bed evolution was averaged at 50 × 50 m grid cells. The land boundaries are shown to delineate the general channel area and are an approximation.

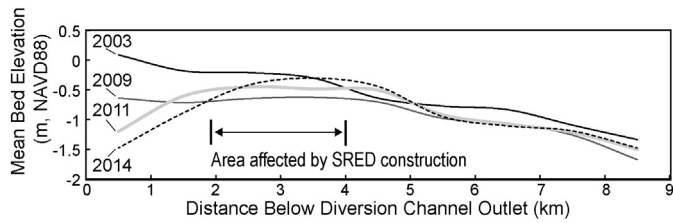


Fig. 7. Observed basin bed elevation. Plot lines are interpolated from averaged values of bathymetric survey data spanning the full basin width and differentiated by distance below the diversion channel outlet.

channel, centrifugal forces pushed the high velocity core differentially toward the outer southern bank. This asymmetry in flow velocity propagated over time (Fig. 13), as the higher velocity flow promoted a lateral gradient in turbulent energy and bed stress that preferentially entrained and transported bed and bank sediment near the southern bank relative to the northern bank. Fig. 14 shows that the predicted locations of high bed stress evolved in a similar pattern as the location of the high velocity core. By 2014, the primary and secondary flow patterns and channel geometry evolved to resemble that in a typical river channel meander bend (Leopold and Wolman, 1960).

Along the upstream section of the northern diversion-channel bank, river flow entering the diversion became horizontally separated from the land boundary because of the sharp angle at which flow was redirected from the main river. Within the separation zone, there was little energy input from the primary current (Ardesch, 2014) and flow circulated slowly in the upstream direction. Model results predicted that this zone increased in size both laterally and longitudinally between 2004 and 2012 and remained stable between 2012 and 2014 (observable in Fig. 10). This predicted increase reduced the fraction of the channel width available to convey flow and sediment into the receiving basin by ~20%. However, model results indicate that the horizontal thickness of the separation zone was variable along the depth profile and thinnest near the channel bed, which is the depth interval where the majority of sand is typically conveyed. These results are aligned with laboratory flume observations of a diversion flow structure reported in Neary and Odgaard (1993), which also found that the flow separation zone thickness decreased with depth.

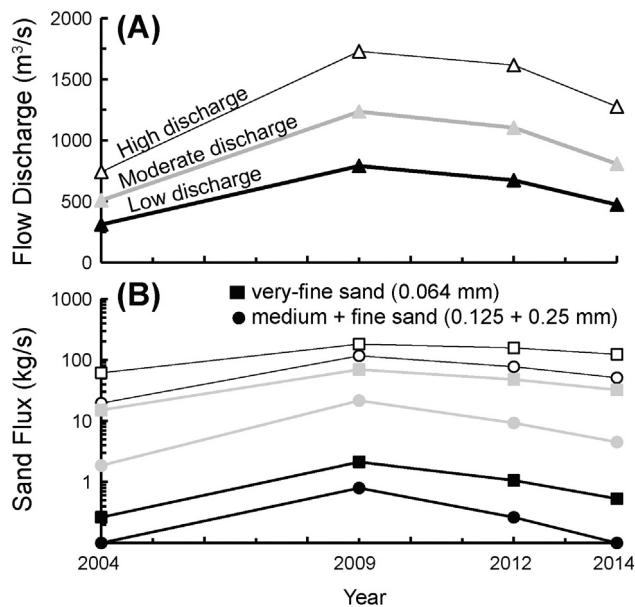


Fig. 8. Modeled (A) flow and (B) sand load entering the diversion channel for the three steady discharges: low ($8800 \text{ m}^3/\text{s}$), moderate ($15,600 \text{ m}^3/\text{s}$), and high ($21,000 \text{ m}^3/\text{s}$) over time. Results are shown for the four time periods that bathymetric information was available.

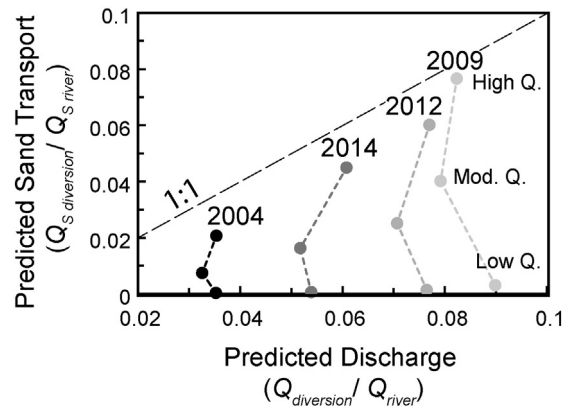


Fig. 9. The fraction of the total river flow and sand load entering the diversion channel as predicted for the four modeled channel and receiving basin bathymetries.

Laboratory experiments by Blanckaert (2009, 2010) and Blanckaert et al. (2013) suggested that flow separation at the inner bank of sharp meander bends, which redirect flow similarly to distributary diversion channels, can significantly reduce the 'effective' channel width and concentrate high-velocity secondary flows toward the toe of the outer bank. Secondary currents generated by sharp-angled meander bends have been shown to be responsible for up to half of the total bed stress and a large percentage of the magnitude of bed material transport within a meander bend (Constantinescu et al., 2013).

Model predictions suggest that flow through the 2004 diversion channel outlet experienced significant flow acceleration as it was forced to constriction through the transition between the relatively deep diversion channel and the relatively shallow receiving basin. The magnitude of the predicted flow acceleration at the diversion outlet decreased monotonically in each successive OBS model run (illustrated in the Fig. 14 bed stress map). This reduced acceleration was likely in response to the observed increases in diversion channel width and upper receiving basin depths which would have reduced flow constriction at the channel-basin transition.

While the evolution of the West Bay diversion-channel morphology played an influential role in determining the predicted flow and sand discharges within the channel, modeling results suggest that it was not the only control. Between 2009 and 2012, the mean cross-sectional area of the channel grew by 37%, and the hydraulic radius was increased by 30%; however, predicted flow discharges decreased an average of 11%. Likely, the gains in transport efficiency promoted by the evolution of the diversion channel were offset by increased receiving basin bed elevation beginning after 2009. During this time period, it was likely that the diversion discharges were responding to [i] the decreased longitudinal gradient between the river and basin surface-water elevations and [ii] the backwater effects propagated by the reduced basin flow depths, which increased the effect of the basin bed roughness and reduced flow velocity. Both of these two processes have the net effect of reducing the energy slope within the diversion channel. Fig. 15 illustrates the predicted reduction in receiving basin flow velocities. The model predicted velocity reductions throughout the basin including the area immediately downstream of the diversion outlet, which experienced monotonic bed erosion (observable in Fig. 7). The relative value of the predicted flow velocities near the diversion correspond to the relative steepness of the energy-water slopes computed within the diversion channel (Table 2).

Between 2012 and 2014, the average predicted diversion discharge was reduced by 26%, while the diversion-channel morphology remained relatively stable except for the reduction in depth of the large scour hole located within the channel bed. It was during this time period that the USACE constructed two additional strips of SRED islands in the upper and middle receiving basin that resulted in a relatively sudden, substantial increase in basin bed elevation. Likely the

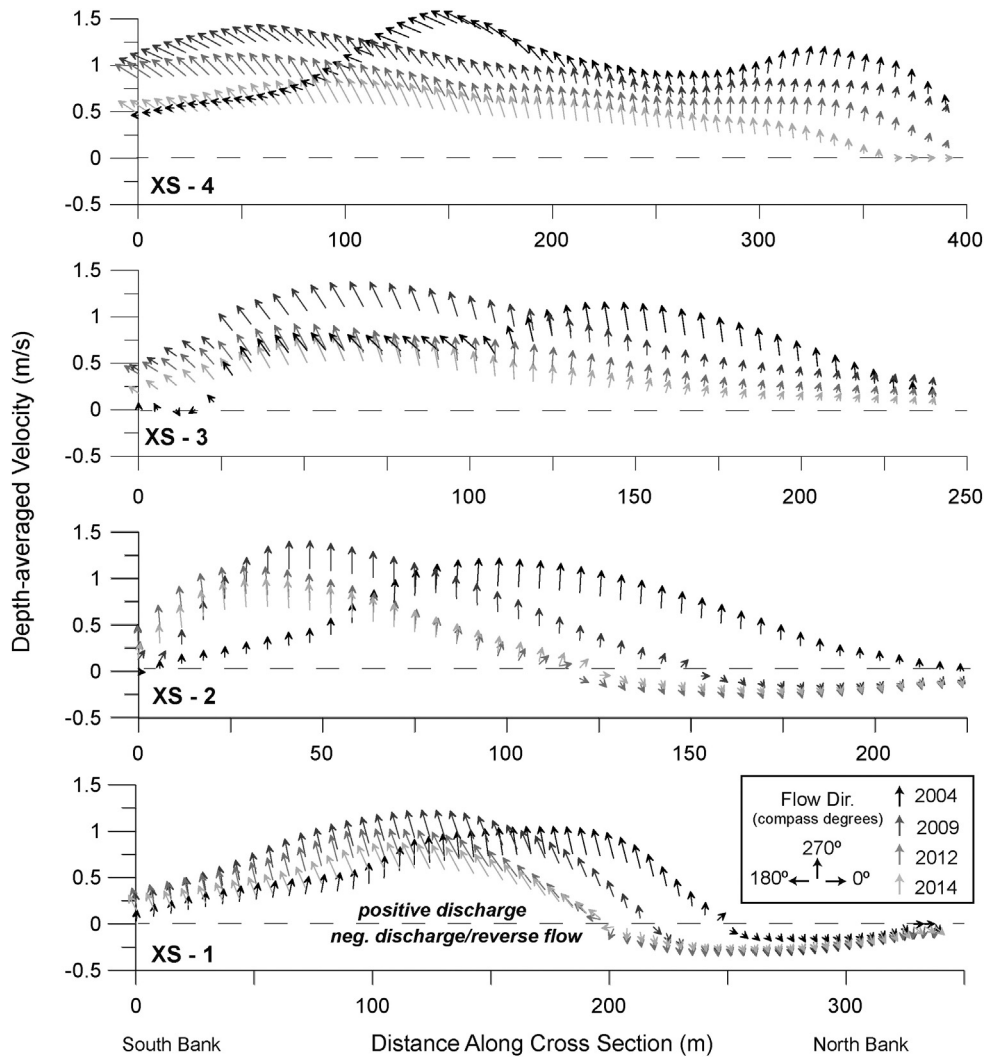


Fig. 10. Depth-averaged horizontal flow velocity through the diversion channel at four cross sections (the locations are shown in Fig. 2) modeled using four bathymetries: 2004, 2009, 2012, and 2014. The arrow direction shows local depth-average flow direction. The velocities were computed by simulating a moderate 16,500 m³/s flow discharge at the upstream river boundary.

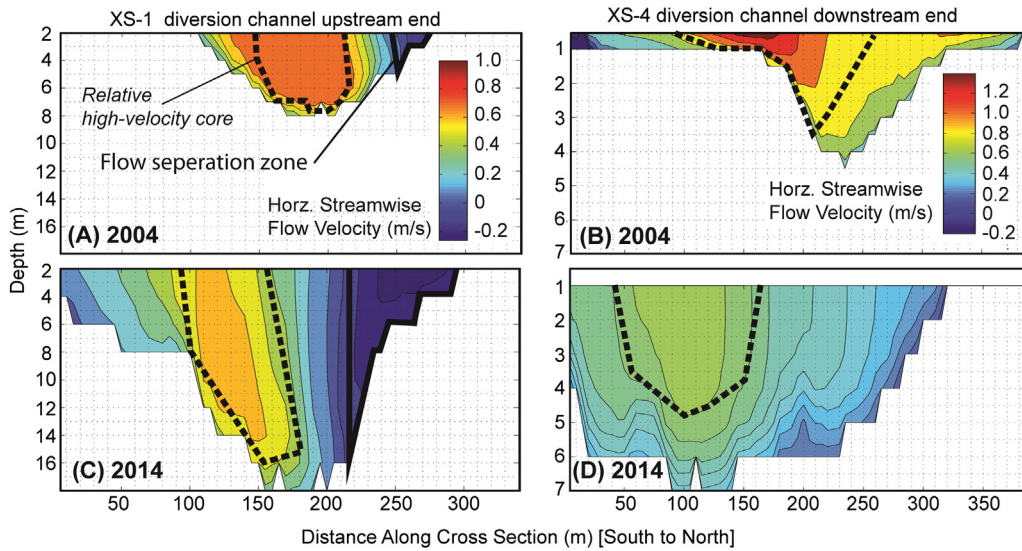


Fig. 11. The modeled velocity distribution for two diversion channel cross sections in 2004 (A and B) and 2014 (C and D). The velocities were computed by simulating a moderate 16,500 m³/s flow discharge at the upstream river boundary. The relative high-velocity core (dashed black line) was calculated as the cross-sectional area containing the top quartile of predicted flow velocities.

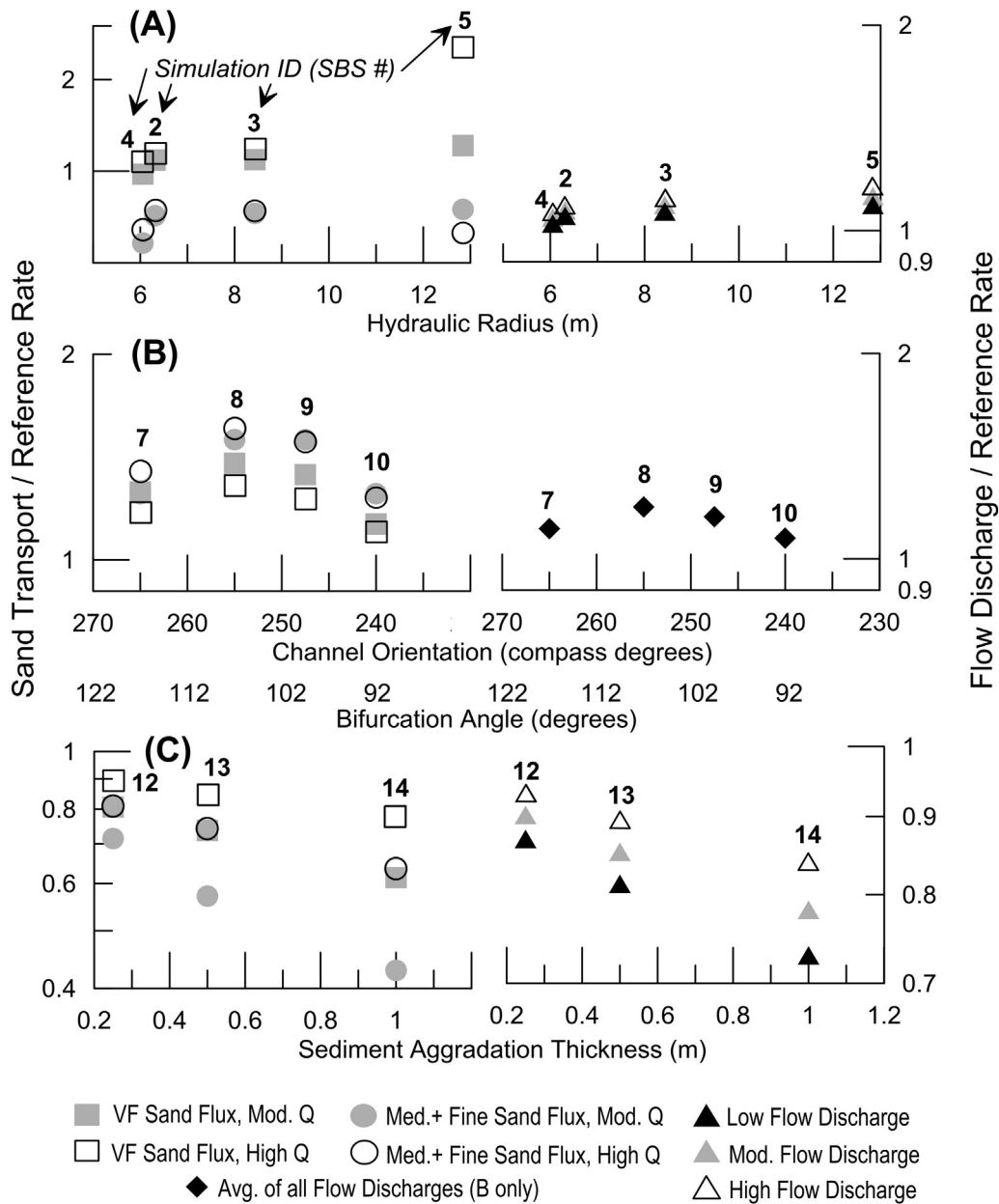


Fig. 12. Flow and sediment transport entering the diversion channel for different modeled scenarios differentiated by (A) diversion channel hydraulic radius, (B) channel orientation, and (C) receiving basin elevation (defined by thickness of sediment aggradation over a base bathymetry). Discharges are shown relative to an initial reference rate (RR). In (A), the RR was computed for a channel with a uniform depth (5 m) and hydraulic radius (3.5 m) (i.e., SBS 1). In (B), the RR was computed for a channel orientation of 270° (i.e., SBS 6). In (C), the RR was computed for the observed 2004 basin bathymetry with zero sediment aggradation (i.e., SBS 11).

presence of the SREDS was the driving influence (up to 50%) of the reduction in flow velocity in the upper basin and in the diversion channel (up to 25%). This general reduction of flow velocity in the channel would have significantly impacted the channel sediment transport capacity and may have initiated the partial infilling of the diversion-channel scour hole.

To more precisely estimate the effect that the SRED island construction had on the flow and sand discharge within the diversion channel, a supplemental Delft3D modeling scenario (i.e., SBS) was executed. In this experimental scenario, the observed 2014 bathymetry was modified by reducing the bed elevation within the subaerial footprint of the SRED islands (see Fig. 1) to -0.5 m NAVD88, which was the approximate mean elevation of the ambient basin bed that was assumed not significantly affected by SRED construction. The model predicted that removal of the SRED islands increased receiving basin flow velocities to near the 2012 (i.e., OBS 3) values and increased the diversion-

channel water-surface slopes to the 2009 (i.e., OBS 2) values. Further, the supplemental model results predicted that the diversion flow increased by 68%, on average, and that the sand transport increased by 260%, on average, relative to the original 2014 (i.e., OBS 4) projections.

5.2. Parsing the effect of morphologic properties on diversion function

The results of the initial observed-bathymetry scenario modeling experiment indicated that the observed morphologic changes significantly altered the predicted discharge of flow and sand transport within the West Bay diversion channel (Fig. 8); however, the experimental results provide little understanding of what aspects of the morphological changes were most responsible for the altered diversion function. Further, the analysis of the modeling results suggest that the properties of the downstream receiving basin can also affect flow and sediment transport within the upstream diversion channel through the

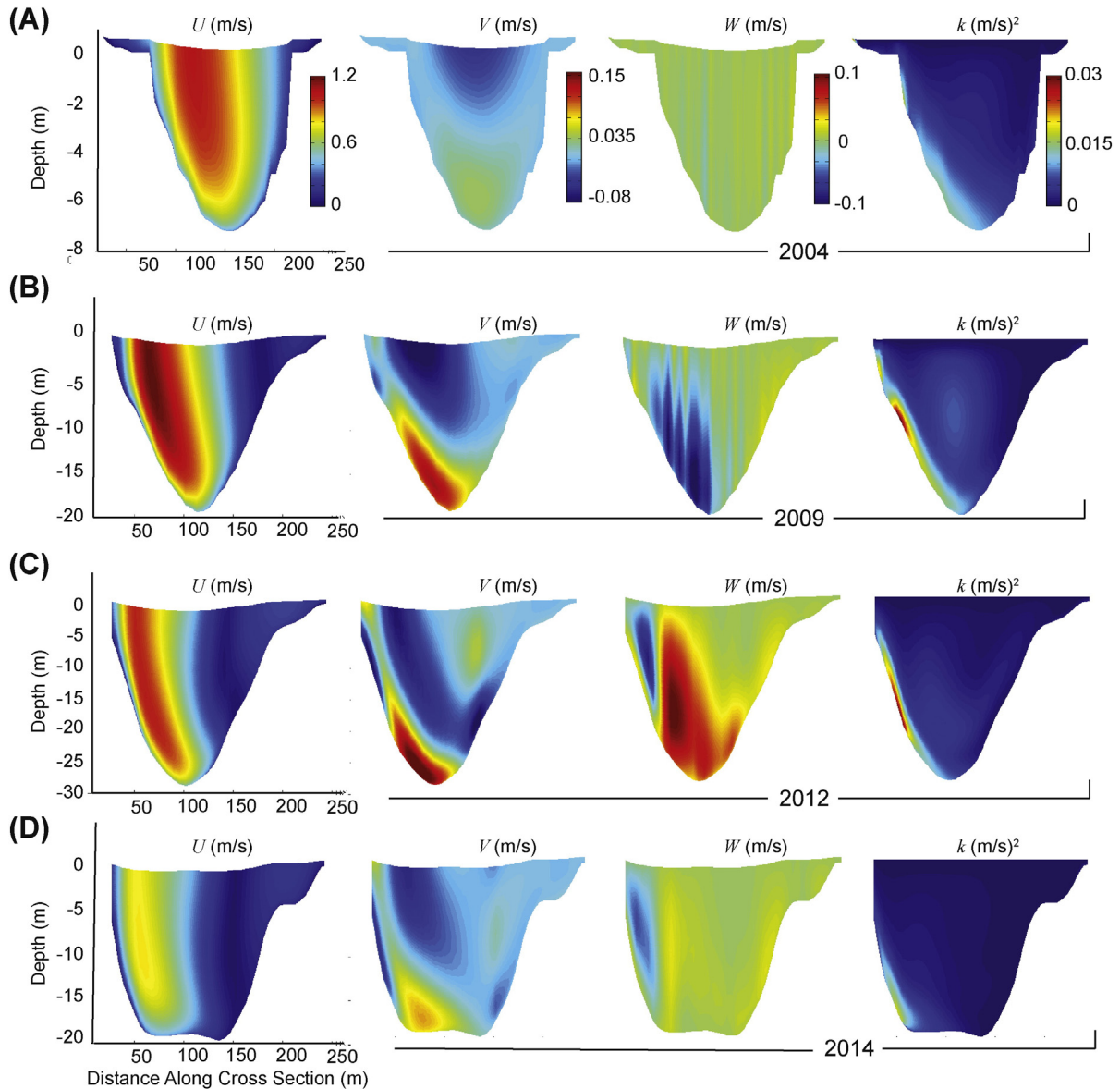


Fig. 13. Modeled flow patterns in XS-3 for (A) 2004, (B) 2009, (C), 2012, and (D) 2014 channel bathymetries during the moderate $15,600 \text{ m}^3/\text{s}$ river discharge. For each bathymetry, downstream (U), transverse (V), vertical (W), and turbulent energy (k) are shown.

production of a significant backwater effect. Analysis of the synthetic-bathymetry scenario results provides a simple means to isolate the relative effect of three specific morphologic properties (i.e., diversion channel hydraulic radius, channel orientation, and basin bed elevation) on flow and sediment transport in the diversion channel.

As observed in Fig. 12, altering the diversion-channel dimensions, in terms of increasing the hydraulic radius, led to a modest increase in flow discharge (<15%). The increased flow corresponded with a similar predicted increase in very-fine sand discharge that may have been a result of the tendency of very-fine sand to travel unstratified in flow (as washload) in the LMR (Ramirez and Allison, 2013). Model results show that the larger R values reduced the constriction of flow passing through the channel and promoted smaller flow velocities (Table 3). The decreased flow velocities likely led to a reduction in discharge of the fine and medium sand passing through the diversion channel. In contrast to the very-fine sand, transport of the coarser sand fractions that remained vertically stratified within the flow column was more dependent on near-bed velocities than total flow discharge.

Altering the angle between the orientation of the main river channel and the diversion channel (i.e., the bifurcation angle) had a nonlinear

effect on the diversion discharges. As illustrated in Fig. 16, while the size of the flow-separation zone along the north bank increases with bifurcation angle, flow velocity along the south bank peaks at a bifurcation angle of 107° , decreasing at higher and lower angles. It is hypothesized that this observation is because of the juxtaposition of two processes: [i] as bifurcation angle increases, flow into the diversion channel is driven less by the inertial forces of the main river current, becoming more reliant on slower, secondary currents, and [ii] as bifurcation angle decreases, flow must pass through a larger length of the diversion footprint before entering the horizontally constrained section of the diversion channel. The bed elevation within the diversion footprint is lower than the proximal channel-bar bed, which causes flow expansion and reduces flow velocity.

The effect of channel orientation on flow and sediment discharge in diversion channels has not been widely studied and remains poorly understood. A recent numerical study by Gaweesh and Meselhe (2016) investigated the effect of diversion channel orientation on fluvial sand capture efficiency for a hypothetical engineered diversion in the LMR. Their results show that altering the bifurcation angle between 30° and 150° can alter capture efficiency by up to 20% (for coarser

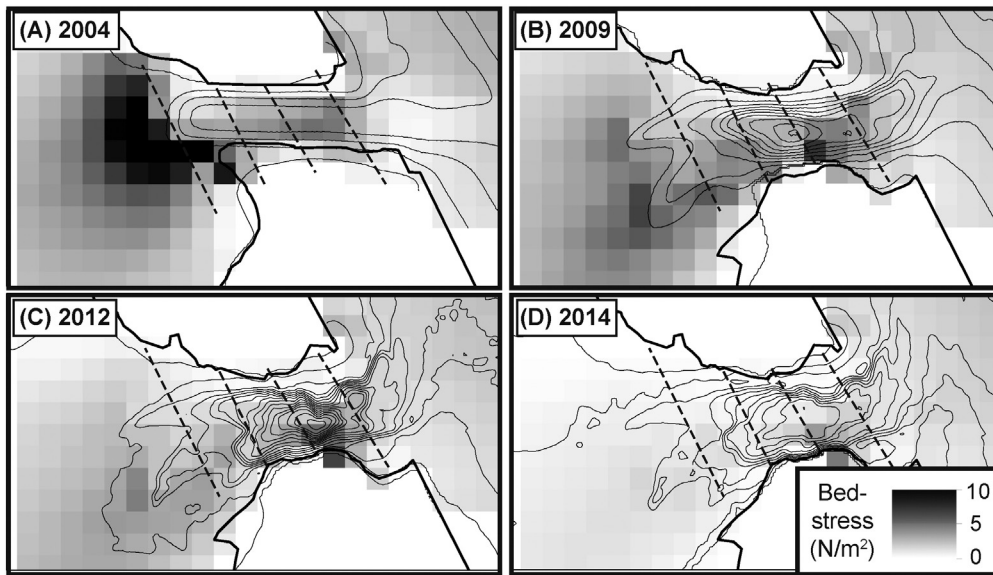


Fig. 14. The spatial distribution of modeled bed stress for four sediment diversion channel bathymetries. Bed stress was computed by simulating a moderate flow discharge at the upstream river boundary. For this plot, bed stress was averaged at 50×50 m grid cells. Contour lines show observed elevation at 2-m intervals. The land boundaries are shown to delineate the general channel area and are an approximation; the location of the four transects (dashed lines) used to analyze flow velocities are also shown for reference.

sands; the capture efficiency of finer sands was less affected) and that the efficiency peaked at angles near 105° . Hardy et al. (2011) also used numerical modeling to investigate the effect of small (relative to the West Bay diversion) bifurcation angles (ranging from 44° to 83°) on flow structure in idealized channels. They found that increasing bifurcation angle had three primary effects on the flow downstream of the bifurcation: [i] channel-averaged flow velocities increased, [ii] near-bank flow velocities increased along the downstream bank (i.e., the bank with the largest radius of curvature), and [iii] the size of the low-velocity flow-separation zone along the upstream bank increased. Garde and Raju (2006) summarized earlier research studies (e.g., Bulle, 1926; Lindner, 1953) that investigated the effect of

bifurcation angle, which ranged from 30° to 150° , on the fraction of bedload sediment captured by diversion channels. Their summary indicated that bedload capture decreases with increasing bifurcation angle until the bifurcation angle exceeds 120° ; as bifurcation angle increases beyond that value, bedload capture increases. From these results, they concluded that the diversion of bedload sediment was dominated by secondary current hydrodynamics. They did not provide any data on suspended sediment transport, which is the dominant sediment transport mode at the West Bay diversion, and hypothesized that the amount of suspended sediment captured by a diversion channel would remain largely independent of bifurcation angle.

The results of the modeling scenarios that simulated the effect of receiving basin aggradation (SBS 11–14) indicate that increased basin-bed elevation had an adverse effect on the diversion-channel discharges. For example, increasing the mean bed elevation by 1 m had a slight impact on flow velocity within the receiving basin (slowing the spatially averaged basin velocity by $\sim 4\%$); however, that same change in bed elevation reduced the spatially averaged diversion channel velocity by 18% (e.g., from 0.55 to 0.45 m/s for the moderate river discharge, $15,600 \text{ m}^3/\text{s}$) and reduced the transport of the fine and medium sand fraction within the diversion channel by nearly 30%. Analysis of the model results suggests that the primary means by which the basin aggradation affected the diversion discharges was through the promotion of an enhanced backwater effect. The model predicted that the reduction in surface-water slope for scenario SBS 12 (+0.25 m), SBS 13 (+0.5 m), and SBS 14 (+1 m) from the initial 2004 value (i.e., 23.1×10^{-5}) was 27%, 37%, and 49%, respectively, for the moderate discharge. For reference, the predicted energy slopes for the OBS are shown in Table 2.

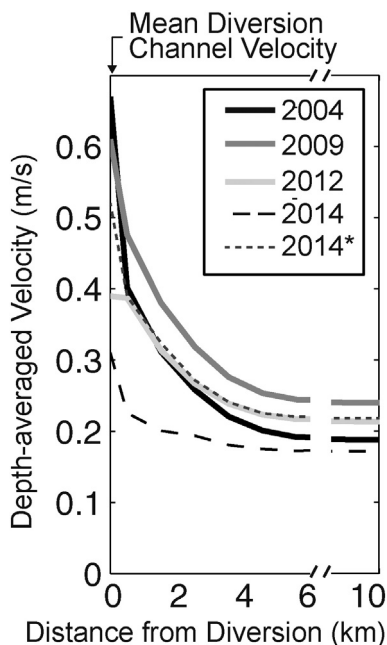


Fig. 15. Predicted receiving basin flow velocities for five different diversion bathymetries at the moderate river discharge. The velocities are spatially averaged and reported by distance away from the diversion-channel outlet. The 2014* velocities were computed during the SBSS scenario, which employed the observed 2014 bathymetry adjusted to remove the morphological effects of the SRED islands.

Table 3
Changes in predicted channel velocities because of altered hydraulic radius values.^a

Scenario ID	R (m)	Channel-avg. vel. (m/s)	Reduction (%)
SBS 1	3.5	0.84	–
SBS 2	6.1	0.64	24
SBS 3	6.3	0.50	40
SBS 4	8.4	0.39	54
SBS 5	12.8	0.24	71

^a Metric values are an average of those calculated from the moderate and high scenario discharges.

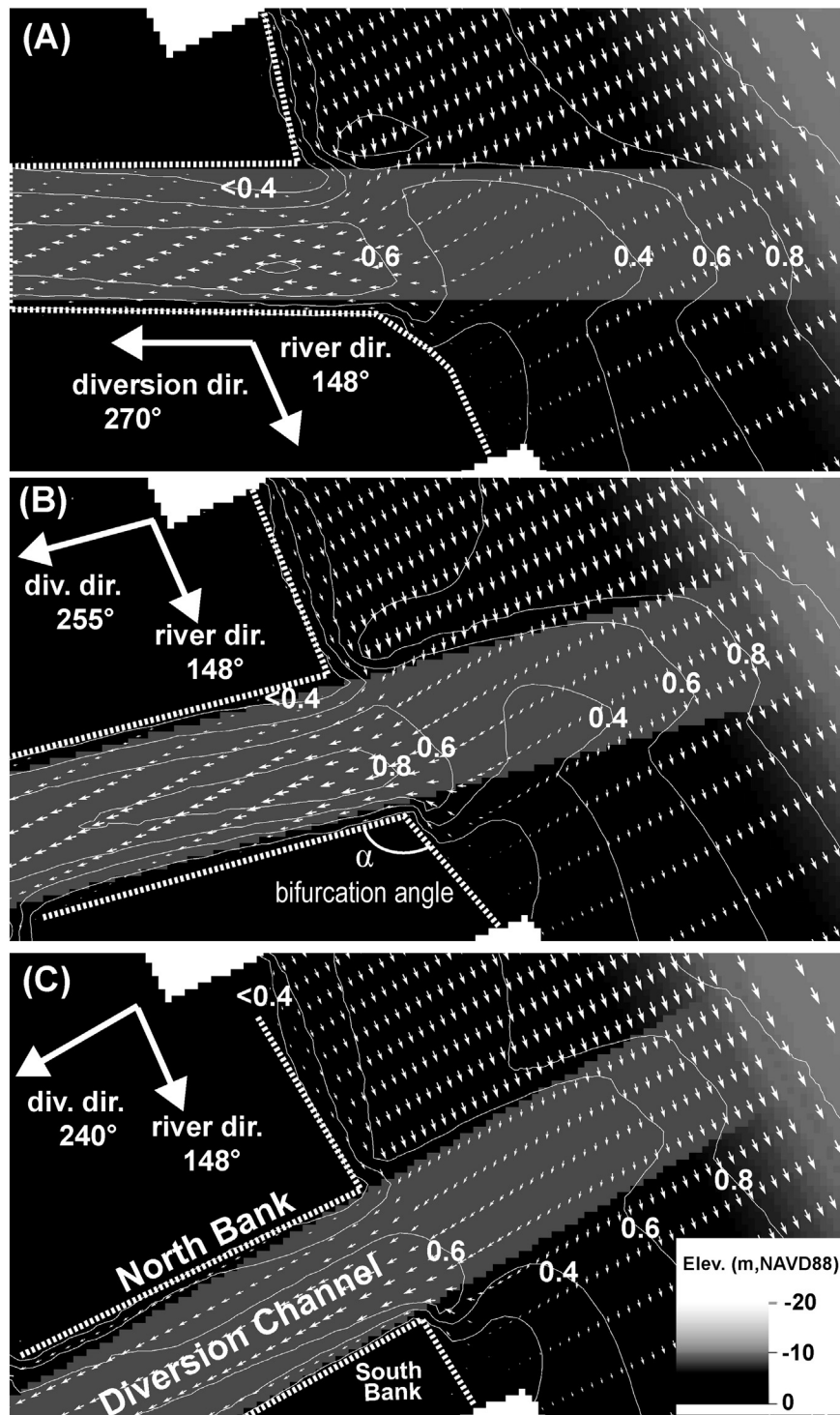


Fig. 16. Modeled patterns of river flow entering the diversion channel for three channel orientations (in compass degrees), (A) 270° ($\alpha = 122^\circ$), (B) 255° ($\alpha = 107^\circ$), and (C) 240° ($\alpha = 92^\circ$) during the moderate river discharge. Relative size and direction of arrows show local depth-averaged flow velocity and direction, respectively. Contour lines are computed for depth-averaged flow velocity at 0.2 m/s intervals.

While the results of the SBS 11–14 model runs illustrate that changes in the receiving basin bed elevation did have a significant impact on the upstream diversion-channel discharges, the magnitudes of the impacts were typically smaller than the changes in the channel discharges predicted during the OBS. This was despite the fact that the ‘observed’ receiving basin bed only aggraded an average of 0.12 m between 2004 and 2014. For comparison, the spatially averaged difference in receiving basin bed elevation between SBS 11 and SBS 14 was 0.44 m. This discrepancy highlights the fact that other morphological properties beyond

mean receiving basin bed elevation must have also significantly impacted the diversion function as predicted in the OBS model runs.

The results of the SSBS (i.e., simulating the 2014 diversion morphology with the effects of the SREDs removed) model run suggest that the spatial distribution of the sediment aggradation within the receiving basin may have a greater impact on the sediment diversion function than the magnitude of the aggradation. In the scenario setup, the removal of the SRED islands lowered the mean basin elevation by 0.14 m; however, the model results predicted that this change reduced

the water-surface slope within the diversion channel by 150% (for the moderate river discharge). As observed in Fig. 1, SRED construction consisted of sediment aggradation in a localized area of the receiving basin. The SBS 14 model run aggraded a larger overall magnitude of sediment, but it was more uniformly distributed in space and only altered the water-surface slope within the diversion channel by 49%.

5.3. A conceptual model of the erosional phase of crevasse-splay evolution using West Bay as an analogue

If the observations of widespread bed erosion and subsequent infilling documented at the West Bay diversion in this study are indicative of the initial phase of crevasse-splay development generally, they provide a useful description of a relatively high-resolution model of landscape evolution. Fig. 17 shows a conceptual diagram of the erosional phase of crevasse-splay evolution based on the data presented in this study and a synthesis of prior research on distributary channels and splay formation. Fig. 17A shows the bed morphology and relative velocity distribution soon after the crevasse is initially formed. Within the initial channel, flow is relatively swift and uniformly distributed; as flow approaches the transition between the crevasse channel (initial depth = 5) and receiving basin (initial depth = 1), the reduction in flow depth causes local acceleration. This accelerated flow will promote bed erosion within the transition area; however, that eroded sediment is quickly deposited upon the proximal basin bed, initially within two channel widths of the channel outlet (Edmonds and Slingerland, 2007), as the transporting flow responds to the slow unconfined

currents within the basin and enhanced bed friction (Wright, 1977; Wellner et al., 2005).

Fig. 17B shows the crevasse channel morphology at the point when the channel bed scour is at a maximum depth. The bed scour resulted from the abundance of swift flow throughout the cross-sectional area of the channel including along the near-bed area; once the channel cross-sectional area reached an equilibrium size relative to the channel flow regime and high-velocity flows were sufficiently removed from the near-bed area, scour would have abated. Depending on the angle at which river flow must be redirected into the diversion channel, centrifugal forces may increase the lateral velocity gradient resulting in meander-like channel evolution and channel reorientation. Erosion at the channel-basin transition would spread basinward until the flow acceleration associated with the loss in flow depth was balanced by flow deceleration introduced by the increase in flow width within the unconfined basin. Upon entering the basin, the width of the river water typically is assumed to spread in accordance to friction-dominated turbulent jet theory (Wright and Coleman, 1974; Wright, 1977; Wellner et al., 2005). Deposition of bed sediment occurs [i] at the lateral margins of the jet creating subaqueous levees and [ii] in the longitudinal downstream direction owing to a decline in 'jet momentum flux', which creates mouth bar formation (Hoyal et al., 2003; Fagherazzi et al., 2015). Flow accelerates over the upstream face of the mouth bar and decelerates over the downstream side causing it to prograde (Edmonds and Slingerland, 2007).

Fig. 17C shows the crevasse channel nearing steady-state, when its morphology has fully evolved to convey its typical flow and sediment loads. Increased channel width and backwater effects caused by

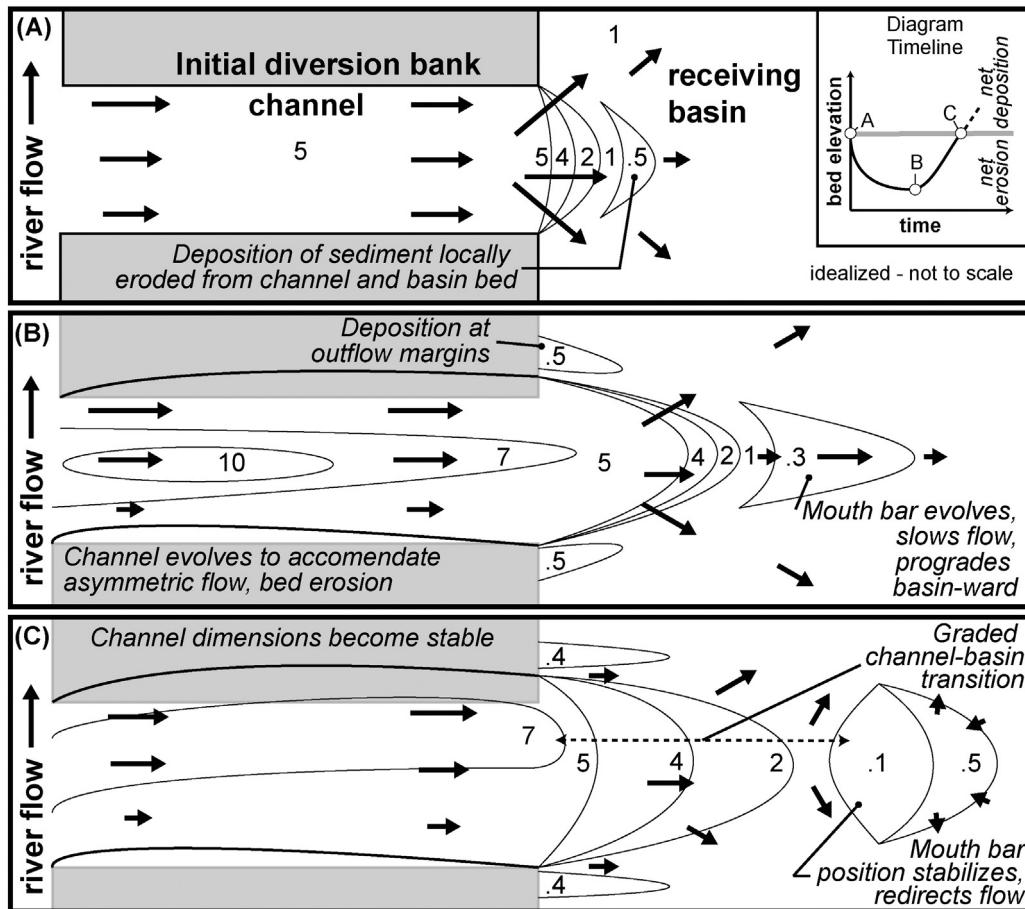


Fig. 17. Conceptual diagram of the initial 'erosional-phase' morphodynamics and evolution of an idealized diversion channel for three time periods, (A) to (C). Arrows indicate depth-averaged flow direction and magnitude (arrow length). Numbers are hypothetical depth below sea level. (A) Initially the diversion channel is straight with a bifurcation angle of 90°. (B) Morphological processes relating to the evolving channel and upper receiving basin dominate land building processes. (C) After the diversion channel evolves dimensions that can efficiently convey the diverted river flow and sediment, the regional bed morphology stabilizes and land building processes may become significant.

downstream sediment aggradation (e.g., mouth bar formation and growth) has further decreased flow velocities (Olariu and Bhattacharya, 2006; Edmonds et al., 2009) and former areas of abrupt scour have infilled to create a more uniform bed bathymetry. The mouth bar has widened and prograded to where its thickness relative to the water depth steers flow around its body rather than accelerating flow over it, which bifurcates the inflow of water and sediment into two pathways (Edmonds and Slingerland, 2007). The mouth bar obstructs flow and forms a low-energy wake on its lee side that encourages further deposition of sediments passing through its margins (Fagherazzi et al., 2015). The majority of the mouth bar at this stage is composed of sediment eroded from the channel and basin bed; however, because bed erosion is now minimal, future mouth bar growth will be dependent on the deposition of diverted river sediment. While no coherent mouth bar is observable in the West Bay data, the theoretical location of mouth bar development is important because it is the region where river-sediment-controlled land building should initiate (Wellner et al., 2005; Esposito et al., 2013; Fagherazzi et al., 2015). The lack of an observed mouth bar may be because of a range of possible processes such as the continued reworking of bed sediment by nonriverine sediment transport drivers such as storm currents and waves (Galloway, 1975; Allison et al., 2000; Nardin and Fagherazzi, 2012). Another possible explanation for the apparent absence of a mouth bar is the lateral diffusion of sediment out of the main advective current exiting the diversion outlet because of the production of turbulence within the jet-like flow (Mariotti et al., 2013). The formation of well-developed subaqueous levees may effectively ‘channelize’ the flow downstream of the diversion outlet, which would preserve momentum and sediment-transport capacity leading to further downstream translation of the final mouth-bar location (Canestrelli et al., 2014). Despite the stabilization of the channel morphology and the assumed initiation of splay development at the conclusion of this stage, areas within the receiving basin may continue to erode locally (Shaw and Mohrig, 2014). For example, new sediment deposition may constrict flow pathways within the basin and lead to spatially abrupt increases in flow velocity and sediment transport capacity. Please note that further discussion about possible mouth bar and splay development in the West Bay receiving basin is provided in the online supplemental information.

5.4. Implication for the design and operation of river sediment diversions

The results of this numerical modeling study provide some guidance for sediment diversion design and operation in fluvial systems similar to the Mississippi River delta (e.g., river-dominated deltas; large, low-slope sandy rivers). While future river sediment diversions may be engineered with controlled river intakes or armored channel beds (e.g., CPRA, 2012), their performance will still depend on their initial dimensions, orientation, and the evolution of the receiving basin morphology. The West Bay sediment-diversion channel experienced significant morphologic evolution soon after initial operation. This evolution was predicted to alter its ability to convey flow and sediment. Initially, between 2004 and 2012, the channel morphology increased in complexity and the flow structure became more asymmetrical. After 2012, the morphology and flow structure became more graded and adopted characteristics similar to that in a natural distributary channel. Changes in channel geometry and orientation likely increased channel conveyance capacity relative to the 2004 diversion channel; however, increased basin bed elevation was likely responsible for decreasing the net channel conveyance capacity by introducing significant backwater effects. While these backwater effects may be unavoidable because a primary objective of a sediment diversion is to aggrade the receiving basin, the spatial patterns of basin aggradation may be manipulated through diversion design to minimize the extent of the backwater effects. For example, future research could investigate the effects of [i] diversion channel and receiving basin size, [ii] the distance between the focus of sediment deposition and the diversion channel outlet, and [iii]

spatially-uniform sediment deposition relative to spatially heterogeneous sediment deposition on the magnitude of the backwater effects and the manner in which they propagate upstream. We should note that despite the fact that increased basin bed elevation may degrade the diversion channel function, it can still produce a net positive effect on land building by increasing the fluvial sediment trap efficiency of the receiving basin and by armoring the basin bed and banks against ocean wave erosion (Allison and Meselhe, 2010; Dean et al., 2014).

6. Conclusions

This study documents the morphological evolution of the West Bay sediment diversion, which was designed to function as a crevasse-splay to build land in the proximal receiving basin. Initially, the diversion channel was built with uniform geometry (~60 m wide, bed elevation = -7.3 m NAVD88). After a decade of conveying diverted river flow and sediment, the channel dimensions increased by 43% in width and 142% in depth. Channel orientation shifted from 275° to 259°, which decreased the bifurcation angle. Bathymetric survey data indicates that by 2009, a large scour hole had developed within the diversion channel and that it grew to a maximum depth near 20 m below the initial channel bed level by the year 2012. Between 2012 and 2014, the scour hole within the diversion had infilled by ~10 m. Numerical modeling predicted that, in response to these changes in channel morphology and the observed sediment aggradation in the receiving basin, the diversion function (in terms of conveying river flow and sediment into the receiving basin) was significantly impacted. The feedback between the observed channel morphology and the predicted channel hydrodynamics illustrates a case study of how an engineered channel evolves and adapts to better convey its typical loads of flow and sediment.

Serving as an analogue for a crevasse-splay, the study of the West Bay diversion offers insight into the initial phase of evolutionary development. During this phase, erosional processes initiate within the crevasse and then eventually subside in favor of depositional processes, at which time splay building is hypothesized to become significant. Study results show how after 5 years of increasing flow and sediment discharge within the diversion channel, the cumulative effects of the observed changes in diversion morphology began to reduce the sediment transport capacity within the diversion area. Study results suggest that after 10 years of diversion operation the channel and basin bed around the diversion site, which was initially erosional, has become primarily depositional. These results [i] appear to confirm previous assumptions about the temporal lag between crevasse and splay development derived from observations (e.g., Boyer et al., 1997; Cahoon et al., 2011) and analysis of relict sedimentary deposits (e.g., Wells and Coleman, 1987; Tooth, 2005) and [ii] provide fine-scale details about the key process that shapes river deltas of all sizes (Wright, 1977; Syvitski et al., 2005). The erosional phase of crevasse-splay development is dependent on the super-elevation of the river surface above the basin water surface or floodplain surface to generate a steep gradient in energy head and high velocities in the water flowing through the crevasse. While this super-elevation is theoretically necessary to cause river flow to overtop the river banks and levee and initiate crevasse incision (Mohrig et al., 2000; Kleinhans et al., 2013), in certain situations (e.g., when the river stage is permanently reduced below the crevasse bed elevation), the erosional phase of crevasse-splay development may be abbreviated.

The results of this study have implications for the design and operation of future river sediment diversions. For uncontrolled sediment diversions, channel morphodynamics may significantly alter the diversion function away from its design specifications. For controlled and uncontrolled diversions, changes in receiving basin morphology, specifically because of sediment aggradation, may affect the diversion function through the production of backwater effects that propagate upstream into the diversion channel. While the backwater effects reduce the sediment transport capacity of the diversion channel, which

reduces the flux of new river sediment available to build land, they may also promote land building by increasing the trapping efficiency of the introduced sediment once it enters the receiving basin from the river.

Acknowledgements

This project was funded in part by the Louisiana Coastal Protection and Restoration Authority (CPRA) Task Orders 15 and 16 and the Water Institute of the Gulf's Science and Engineering Plan (SEP). Cyndhia Ramatchandirane, Dallan Weathers, and Mike Ramirez provided invaluable support to this study. Alex Kolker (LUMCON) and his crew of graduate students provided significant aid during data collection activities. The USACE Coastal and Hydraulics Lab and New Orleans District provided much of the pre-2012 raw data analyzed in this study. Reviews by Maarten Kleinhans and two anonymous reviewers greatly improved the clarity and substance of this manuscript. The journal editor provided exceptional editorial assistance during the review process.

Appendix A. Supplementary data

The online supplemental material includes detailed information on numerical model parameterization and calibration, numerical model calibration results, and analysis of splay building interpreted from the 2014 bathymetric survey. Supplementary data associated with this article can be found in the online version, at <http://dx.doi.org/10.1016/j.geomorph.2016.02.005>.

References

- Allen, J.R.L., 1964. Studies in Fluvial sedimentation: six cyclothem from the Lower Old Red Sandstone, Anglo-Welsh Basin. *Sedimentology* 3, 163–198.
- Allison, M.A., Meselhe, E.A., 2010. The use of large water and sediment diversions in the lower Mississippi River (Louisiana) for coastal restoration. *J. Hydrol.* 387 (3), 346–360.
- Allison, M.A., Kineke, G.C., Gordon, E.S., Goñi, M.A., 2000. Development and reworking of a seasonal flood deposit on the inner continental shelf off the Atchafalaya River. *Cont. Shelf Res.* 20, 2267–2294. [http://dx.doi.org/10.1016/S0278-4343\(00\)00070-4](http://dx.doi.org/10.1016/S0278-4343(00)00070-4).
- Allison, M.A., Demas, C.R., Ebersole, B.A., Kleiss, B.A., Little, C.D., Meselhe, E.A., Powell, N.J., Pratt, T.C., Vosburg, B.A., 2012. A water and sediment budget for the lower Mississippi–Atchafalaya River in flood years 2008–2010: implications for sediment discharge to the oceans and coastal restoration in Louisiana. *J. Hydrol.* 432, 84–97.
- Allison, M.A., Vosburg, B.M., Ramirez, M.T., Meselhe, E.A., 2013. Mississippi River channel response to the Bonnet Carré Spillway opening in the 2011 flood and its implications for the design and operation of river diversions. *J. Hydrol.* 477, 104–118.
- Allison, M.A., Ramirez, M.T., Meselhe, E.A., 2014. Diversion of Mississippi River water downstream of New Orleans, Louisiana, USA to maximize sediment capture and ameliorate coastal land loss. *Water Resour. Manag.* 28 (12), 4113–4126.
- Andrus, T.M., 2007. Sediment Flux and Fate in the Mississippi River Diversion at West Bay: Observation Study (M.S. Thesis) Louisiana State University, Baton Rouge, LA.
- Ardesch, R., 2014. Flow Separation in Sharp-bend-flow (M.Sc. Thesis) Universiteit Utrecht (69 pp.).
- Barras, J.A., Padgett, W.C., Sanders, C.B., 2009. Aerial and Bathymetric Spatial Change Analysis of the West Bay Sediment Diversion Receiving Area. Louisiana for U.S. Army Engineer District, New Orleans (MVN) Report US Army Corps of Engineers (39 pp.).
- Bentley, S.J., Freeman, A.M., Willson, C.S., Cable, J.E., Giosan, L., 2014. Using what we have: optimizing sediment management in Mississippi River delta restoration to improve the economic viability of the nation. Perspectives on the Restoration of the Mississippi Delta. Springer, Netherlands, pp. 85–97.
- Blanckaert, K., 2009. Saturation of curvature induced secondary flow, energy losses and turbulence in sharp open-channel bends. Laboratory experiments, analysis and modelling. *J. Geophys. Res. Earth Surf.* 114, F03015. <http://dx.doi.org/10.1029/2008JF001137>.
- Blanckaert, K., 2010. Topographic steering, flow recirculation, velocity redistribution and bed deformation in sharp meander bends. *Water Resour. Res.* 46, W09506. <http://dx.doi.org/10.1029/2009WR008303>.
- Blanckaert, K., Kleinhans, M.G., McLelland, S.J., Uijttewaai, W.S.J., Murphy, B.J., Kruijs, A., Parsons, D.R., Qiuwen Chen, Q., 2013. Flow separation at the inner (convex) and outer (concave) banks of constant-width and widening open-channel bends. *Earth Surf. Process. Landf.* 38 (7), 696–716.
- Blum, M.D., Roberts, H.H., 2009. Drowning of the Mississippi Delta due to insufficient sediment supply and global sea-level rise. *Nat. Geosci.* 2 (7), 488–491.
- Boustany, R.G., 2010. Estimating the benefits of freshwater introduction into coastal wetland ecosystems in Louisiana: nutrient and sediment analyses. *Ecol. Restor.* 28 (2), 160–174.
- Boyer, M.E., Harris, J.O., Turner, R.E., 1997. Constructed crevasses and land gain in the Mississippi River Delta. *Restor. Ecol.* 5 (1), 85–92.
- Bridge, J.S., 1984. Large-scale facies sequences in alluvial overbank environments. *J. Sediment. Res.* 54 (2), 583–588.
- Bristow, C.S., Skelly, R.L., Ethridge, F.G., 1999. Crevasse splays from the rapidly aggrading, sand-bed, braided Niobrara River, Nebraska: effect of base-level rise. *Sedimentology* 46 (6), 1029–1048.
- Bulle, H., 1926. Untersuchungen über die geschiebeableitung bei der spaltung von Wasserläufen. Forschungsarbeiten auf dem Gebiete des Ingenieurwesens 282, 57–84 (in German).
- Cahoon, D.R., White, D.A., Lynch, J.C., 2011. Sediment infilling and wetland formation dynamics in an active crevasse splay of the Mississippi River delta. *Geomorphology* 131 (3), 57–68.
- Canestrelli, A., Nardin, W., Edmonds, D., Fagherazzi, S., Slingerland, R., 2014. Importance of frictional effects and jet instability on the morphodynamics of river mouth bars and levees. *J. Geophys. Res. Oceans* 119 (1), 509–522.
- Carter, B., 2003. Monitoring Plan for West Bay Sediment Diversion. Louisiana Department of Natural Resources, Coastal Restoration and Management (12 pp.).
- Coleman, J.M., Gagliano, S.M., 1964. Cyclic sedimentation in the Mississippi River deltaic plain. *Gulf Coast Assoc. Geol. Soc. Trans.* 14, 67–80.
- Coleman, J.M., Gagliano, S.M., Morgan, J.P., 1969. Mississippi River subdeltas, natural models of deltaic sedimentation. *Coastal Studies Institute Bulletin* 3. Louisiana State University, Baton Rouge, Louisiana, pp. 23–27.
- Coleman, J.M., Roberts, H.R., Stone, G.W., 1998. Mississippi River Delta: an overview. *J. Coast. Res.* 14 (3), 698–716.
- Constantinescu, G., Kashyap, S., Tokyay, T., Rennie, C.D., Townsend, R.D., 2013. Hydrodynamic processes and sediment erosion mechanisms in an open channel bend of strong curvature with deformed bathymetry. *J. Geophys. Res. Earth Surf.* 118 (2), 480–496.
- CPRA (Coastal Protection and Restoration Authority), 2012. Louisiana's Comprehensive Master Plan for a Sustainable Coast. Baton Rouge, State of Louisiana (190 pp.).
- CPRA (Coastal Protection and Restoration Authority) Fact Sheet, 2009h. Louisiana Coastal Wetlands Conservation and Restoration Task Force West Bay Sediment Diversion (MR-03). Accessed at <http://lacoast.gov/reports/project/West%20Bay%20Fact%20Sheet%2007%20July%202009.pdf>, on September 12th, 2015, 2 pp.
- Day, J.W., Boesch, D.F., Clairain, E.J., Kemp, G.P., Laska, S.P., Mitsch, W.J., Orth, K., Mashriq, H., Reed, D.J., Shabman, L., Simenstad, C.A., Streever, B.J., Twilley, R.R., Watson, C., Wells, J.T., Whigham, D.F., 2007. Restoration of the Mississippi Delta: Lessons from Hurricanes Katrina and Rita. *Science* 315 (5819), 1679–1684.
- Dean, R.G., Wells, J.T., Fernando, H.J., Goodwin, P., 2014. Sediment diversions on the lower Mississippi river: insight from simple analytical models. *J. Coast. Res.* 30 (1), 13–29.
- DeLuca, B.G., 2014. USACE Perspective on Mississippi River Sediment Diversions. Presentation to the Water Institute of the Gulf on behalf of the USACE Mississippi Valley Division, Mississippi River Commission on January 2014, archived at: http://thewaterinstitute.cdn.zcomm.com/userfiles/file/DeLuca_USACE.pdf.
- Edmonds, D., Slingerland, R., 2007. Mechanics of river mouth bar formation: implications for the morphodynamics of delta distributary networks. *J. Geophys. Res. Earth Surf.* 112. <http://dx.doi.org/10.1029/2006JF000574>.
- Edmonds, D.A., Hoyal, D.C., Sheets, B.A., Slingerland, R.L., 2009. Predicting delta avulsions: Implications for coastal wetland restoration. *Geology* 37 (8), 759–762.
- Edwards, T.K., Glysson, G.D., 1988. Field methods for measurement of fluvial sediment. U.S. Geological Survey Open-File Report, pp. 86–531.
- Esposito, C.R., Georgiou, I.Y., Kolker, A.S., 2013. Hydrodynamic and geomorphic controls on mouth bar evolution. *Geophys. Res. Lett.* 40 (8), 1540–1545.
- Fagherazzi, S., Edmonds, D.A., Nardin, W., Leonardi, N., Canestrelli, A., Falcini, F., Jerolmack, D., Mariotti, G., Rowland, J.C., Slingerland, R.L., 2015. Dynamics of river mouth deposits. *Rev. Geophys.* <http://dx.doi.org/10.1002/2014RG000451>.
- Falcini, F., Khan, N.S., Macelloni, L., Horton, B.P., Lutken, C.B., McKee, K.L., Colelle, R.S., Li, C., Volpe, G., D'Emidio, M., Salusti, A., Jerolmack, D.J., 2012. Linking the historic 2011 Mississippi River flood to coastal wetland sedimentation. *Nat. Geosci.* 5 (11), 803–807.
- Fielding, C.R., Crane, R.C., 1987. An application of statistical modeling to the prediction of hydrocarbon recovery factors in fluvial reservoir sequences. In: Ethridge, F.G., Flores, R.M., Harvey, M.D. (Eds.), Recent Developments in Fluvial Sedimentology: SEPM, Special Publication. 39, pp. 321–327.
- Florsheim, J.L., Mount, J.F., 2002. Restoration of floodplain topography by sand-splay complex formation in response to intentional levee breaches, Lower Cosumnes River, California. *Geomorphology* 44 (1), 67–94.
- Galler, J.J., Allison, M.A., 2008. Estuarine controls on fine-grained sediment storage in the Lower Mississippi and Atchafalaya Rivers. *Geol. Soc. Am. Bull.* 120 (3–4), 386–398.
- Galloway, W.E., 1975. Process framework for describing the morphologic and stratigraphic evolution of deltaic depositional systems. *Deltas: Models for Exploration*. Houston Geological Society, pp. 87–98.
- Garde, R.J., Raju, K.R., 2006. Mechanics of Sediment Transportation and Alluvial Stream Problems. New Age International Publishers, New Delhi, India (693 pp.).
- Gaweesh, A., Meselhe, E., 2016. Evaluation of sediment diversion design attributes and their impact on the capture efficiency. *J. Hydraul. Eng.* [http://dx.doi.org/10.1061/\(ASCE\)HY.1943-7900.0001114](http://dx.doi.org/10.1061/(ASCE)HY.1943-7900.0001114).
- Gundersø, R., Egeland, O., 1990. SESIMIRA—a new geological tool for 3D modelling of heterogeneous reservoirs. North Sea Oil and Gas Reservoirs—II. Springer, Netherlands, pp. 363–371.
- Hardy, R.J., Lane, S.N., Yu, D., 2011. Flow structures at an idealized bifurcation: a numerical experiment. *Earth Surf. Process. Landf.* 36 (15), 2083–2096.
- Henderson, F.M., 1966. Open Channel Flow. Macmillan Publishing Co., Inc., New York, NY.
- Hoyal, D.C.J.D., Van Wagoner, J.C., Adair, N.L., Deffenbaugh, M., Li, D., Sun, T., Huh, C., Giffin, D.E., 2003. Sedimentation from jets: a depositional model for clastic deposits of all scales and environments. American Association of Petroleum Geologists Annual Meeting Extended Abstract (6 pp.).
- Jerolmack, D.J., Mohrig, D., 2007. Conditions for branching in depositional rivers. *Geology* 35 (5), 463–466.

- Kellerhals, R., Church, M., Davies, L.B., 1979. Morphological effects of interbasin river diversions. *Can. J. Civ. Eng.* 6 (1), 18–31.
- Kemp, G.P., Day, J.W., Freeman, A.M., 2014. Restoring the sustainability of the Mississippi River Delta. *Ecol. Eng.* 65, 131–146.
- Kim, W., Mohrig, D., Twilley, R., Paola, C., Parker, G., 2009. Is it feasible to build new land in the Mississippi River Delta? *EOS Trans. Am. Geophys. Union* 90 (42), 373–374.
- Kleinbans, M.G., Jagers, H.R.A., Mosselman, E., Sloff, C.J., 2008. Bifurcation dynamics and avulsion duration in meandering rivers by one-dimensional and three-dimensional models. *Water Resour. Res.* 44 (8). <http://dx.doi.org/10.1029/2007WR005912>.
- Kleinbans, M.G., Weerts, H.J.T., Cohen, K.M., 2010. Avulsion in action: Reconstruction and modelling sedimentation pace and upstream flood water levels following a Medieval tidal-river diversion catastrophe (Biesbosch, The Netherlands, 1421–1750AD). *Geomorphology* 118 (1), 65–79.
- Kleinbans, M.G., Haas, T.D., Lavooi, E., Makaske, B., 2012. Evaluating competing hypotheses for the origin and dynamics of river anastomosis. *Earth Surf. Process. Landf.* 37 (12), 1337–1351.
- Kleinbans, M.G., Ferguson, R.I., Lane, S.N., Hardy, R.J., 2013. Splitting rivers at their seams: bifurcations and avulsion. *Earth Surf. Process. Landf.* 38 (1), 47–61.
- Kolker, A.S., Miner, M.D., Weathers, H.D., 2012. Depositional dynamics in a river diversion receiving basin: the case of the West Bay Mississippi River diversion. *Estuar. Coast. Shelf Sci.* 106, 1–12.
- Lane, R.R., Day, J.W., Kemp, G.P., Demcheck, D.K., 2001. The 1994 experimental opening of the Bonnet Carre spillway to divert Mississippi River water into Lake Pontchartrain, Louisiana. *Ecol. Eng.* 17 (4), 411–422.
- Leopold, L.B., Wolman, M.G., 1960. River meanders. *Geol. Soc. Am. Bull.* 71 (6), 769–793.
- Lesser, G.R., Roelvink, J.A., Van Kester, J.A.T.M., Stelling, G.S., 2004. Development and validation of a three-dimensional morphological model. *Coast. Eng.* 51 (8), 883–915.
- Lindner, C.P., 1953. Diversions from alluvial stream. *Trans. Am. Soc. Civ. Eng.* 119A.
- Makaske, B., Smith, D.G., Berendsen, H.J., 2002. Avulsions, channel evolution and floodplain sedimentation rates of the anastomosing upper Columbia River, British Columbia, Canada. *Sedimentology* 49 (5), 1049–1071.
- Mariotti, G., Falcini, F., Geleynse, N., Guala, M., Sun, T., Fagherazzi, S., 2013. Sediment eddy diffusivity in meandering turbulent jets: implications for levee formation at river mouths. *J. Geophys. Res. Earth Surf.* 118 (3), 1908–1920.
- Matsubara, Y., Howard, A.D., 2014. Modeling planform evolution of a mud-dominated meandering river: Quinn River, Nevada, USA. *Earth Surf. Process. Landf.* 39 (10), 1365–1377.
- Meselhe, E.A., Georgiou, I., Allison, M.A., McCorquodale, J.A., 2012. Numerical modeling of hydrodynamics and sediment transport in lower Mississippi at a proposed delta building diversion. *J. Hydrol.* 472, 340–354.
- Mohrig, D., Heller, P.L., Paola, C., Lyons, W.J., 2000. Interpreting avulsion process from ancient alluvial sequences: Guadalupe-Matarranya system (northern Spain) and Wasatch Formation (western Colorado). *Geol. Soc. Am. Bull.* 112 (12), 1787–1803.
- Mossa, J., 1996. Sediment dynamics of the lowermost Mississippi River. *Eng. Geol.* 45, 457–479. [http://dx.doi.org/10.1016/S0013-7952\(96\)00026-9](http://dx.doi.org/10.1016/S0013-7952(96)00026-9).
- Nardin, W., Fagherazzi, S., 2012. The effect of wind waves on the development of river mouth bars. *Geophys. Res. Lett.* 39 (12). <http://dx.doi.org/10.1029/2012GL051788>.
- Neary, V.S., Odgaard, A.J., 1993. Three-dimensional flow structure at open-channel diversions. *J. Hydraul. Eng.* 119 (11), 1223–1230.
- Nittrouer, J.A., Mohrig, D., Allison, M., 2011. Punctuated sand transport in the lowermost Mississippi River. *J. Geophys. Res. Earth Surf.* 116 (F4). <http://dx.doi.org/10.1029/2011JF002026>.
- Nittrouer, J.A., Best, J.L., Brantley, C., Cash, R.W., Czapiga, M., Kumar, P., Parker, G., 2012. Mitigating land loss in coastal Louisiana by controlled diversion of Mississippi River sand. *Nat. Geosci.* 5 (8), 534–537.
- North, C.P., Davidson, S.K., 2012. Unconfined alluvial flow processes: recognition and interpretation of their deposits, and the significance for palaeogeographic reconstruction. *Earth Sci. Rev.* 111 (1), 199–223.
- O'Brien, P.E., Wells, A.T., 1986. A small, alluvial crevasse splay. *J. Sediment. Res.* 56 (6), 876–879.
- Olariu, C., Bhattacharya, J.P., 2006. Terminal distributary channels and delta front architecture of river-dominated delta systems. *J. Sediment. Res.* 76 (2), 212–233.
- Paola, C., Twilley, R.R., Edmonds, D.A., Kim, W., Mohrig, D., Parker, G., Voller, V.R., 2011. Natural processes in delta restoration: Application to the Mississippi Delta. *Ann. Rev. Mar. Sci.* 3, 67–91.
- Peyronnin, N., Green, M., Richards, C.P., Owens, A., Reed, D., Chamberlain, J., Groves, D.G., Rhinehart, W.K., Belhadjali, K., 2013. Louisiana's 2012 coastal master plan: overview of a science-based and publicly informed decision-making process. *J. Coast. Res.* 67 (SP 1), 1–15.
- Pizzuto, J.E., 1987. Sediment diffusion during overbank flows. *Sedimentology* 34 (2), 301–317.
- Ramirez, M.T., Allison, M.A., 2013. Suspension of bed material over sand bars in the Lower Mississippi River and its implications for Mississippi delta environmental restoration. *J. Geophys. Res. Earth Surf.* 118 (2), 1085–1104.
- Roberts, H.H., 1997. Dynamic changes of the Holocene Mississippi River delta plain: the delta cycle. *J. Coast. Res.* 605–627.
- Sadler, P.M., 1981. Sediment accumulation rates and the completeness of stratigraphic sections. *J. Geol.* 569–584.
- Schuurman, F., Kleinbans, M.G., 2015. Bar dynamics and bifurcation evolution in a modelled braided sand-bed river. *Earth Surf. Process. Landf.* 40 (10), 1318–1333.
- Sharp, J., Little, C., Brown, G., Pratt, T., Health, R., Hubbard, L., Pinkard, F., Martin, K., Clifton, N., Perkey, D., Ganesh, N., 2013. West Bay Sediment Diversion Effects. ERDC/CHL TR-13-15US Army Corps of Engineers, Engineer Research and Development Center, Vicksburg, MS (274 pp.).
- Shaw, J.B., Mohrig, D., 2014. The importance of erosion in distributary channel network growth, Wax Lake Delta, Louisiana, USA. *Geology* 42 (1), 31–34.
- Slingerland, R., Smith, N.D., 1998. Necessary conditions for a meandering-river avulsion. *Geology* 26 (5), 435–438.
- Sloff, K., Mosselman, E., 2012. Bifurcation modelling in a meandering gravel-sand bed river. *Earth Surf. Process. Landf.* 37 (14), 1556–1566.
- Smith, D.G., Smith, N.D., 1980. Sedimentation in anastomosed river systems: Examples from alluvial valley near Bannf, Alberta. *J. Sediment. Res.* 50 (1), 157–164.
- Snedden, G.A., Cable, J.E., Swarzenski, C., Swenson, E., 2007. Sediment discharge into a subsiding Louisiana deltaic estuary through a Mississippi River diversion. *Estuar. Coast. Shelf Sci.* 71 (1), 181–193.
- Stouthamer, E., 2001. Sedimentary products of avulsions in the Holocene Rhine-Meuse Delta, the Netherlands. *Sediment. Geol.* 145 (1), 73–92.
- Stouthamer, E., Berendsen, H.J.A., 2001. Avulsion frequency, avulsion duration, and interavulsion period of Holocene channel belts in the Rhine-Meuse delta, the Netherlands. *J. Sediment. Res.* 71 (4), 589–598.
- Strong, N., Paola, C., 2008. Valleys that never were: time surfaces versus stratigraphic surfaces. *J. Sediment. Res.* 78 (8), 579–593.
- Syvitski, J.P., Kettner, A.J., Correggiari, A., Nelson, B.W., 2005. Distributary channels and their impact on sediment dispersal. *Mar. Geol.* 222, 75–94.
- Thorne, C.R., Harmar, O.P., Wallerstein, N., 2000. Sediment Transport in the Lower Mississippi River. Final Report Submitted to U.S. Army Research, Development, and Standardisation Group, London, U.K. (71 pp.).
- Tooth, S., 2005. Splay formation along the lower reaches of ephemeral rivers on the Northern Plains of arid central Australia. *J. Sediment. Res.* 75 (4), 636–649.
- Turner, R.E., Boyer, M.E., 1997. Mississippi River diversions, coastal wetland restoration/creation and an economy of scale. *Ecol. Eng.* 8 (2), 117–128.
- Tye, R.S., Coleman, J.M., 1989. Evolution of Atchafalaya lacustrine deltas, south-central Louisiana. *Sediment. Geol.* 65 (1), 95–112.
- van Rijn, L.C., Roelvink, J.A., Horst, W.Y., 2001. Approximation formulae for sand transport by currents and waves and implementation in DELFT-MOR. Tech. Rep. Z3054.20/40 WL Delft Hydraulics, Delft, The Netherlands (44 pp.).
- Wamsley, T.V., 2013. Land building models: uncertainty in and sensitivity to input parameters. No. ERDC/CHL CHETN-VI-44. Engineer Research and Development Center, Coastal and Hydraulics Lab, Vicksburg, MS 25 pp.
- Wang, H., Steyer, G.D., Couvillion, B.R., Rybczyk, J.M., Beck, H.J., Sleavin, W.J., Meselhe, E., Allison, M.A., Boustany, R.G., Fischenich, C.J., Rivera-Monroy, V.H., 2014. Forecasting landscape effects of Mississippi River diversions on elevation and accretion in Louisiana deltaic wetlands under future environmental uncertainty scenarios. *Estuar. Coast. Shelf Sci.* 138, 57–68.
- Welder, F.A., 1959. Processes of deltaic sedimentation in the lower Mississippi River. Coastal Institute Technical Report 12 C597. Louisiana State University, Baton Rouge, Louisiana (90 pp.).
- Wellner, R., Beaubouef, R., Wagoner, J.A., Roberts, H., Sun, T., 2005. Jet-plume depositional bodies—the primary building blocks of Wax Lake delta. *Gulf Coast Assoc. Geol. Soc. Trans.* 55, 867–909.
- Wells, J.T., Coleman, J.M., 1987. Wetland loss and the subdelta life cycle. *Estuar. Coast. Shelf Sci.* 25 (1), 111–125.
- Wright, L.D., 1977. Sediment transport and deposition at river mouths: a synthesis. *GSA Bull.* 88, 857–868.
- Wright, L.D., Coleman, J.M., 1974. Mississippi River mouth processes: effluent dynamics and morphologic development. *J. Geol.* 82 (6), 751–778.